AD-762 579

PRELIMINARY DESIGN OF A FOA CRYPTO-STEADY ENERGY SEPARATOR FOR USE IN SUPERSONIC AIRCRAFT

David Sobel, et al

George Washington University

Prepared for:

Naval Air Systems Command

September 1972

DISTRIBUTED BY:

NTIS

National Technical Information Service
U. S. DEPARTMENT OF COMMERCE
5285 Port Royal Road, Springfield Va. 22151

TR-ES-724

AD 762579

PRELIMINARY DESIGN OF A FOA CRYPTOSTEADY ENERGY SEPARATOR FOR USE IN SUPERSONIC AIRCRAFT

By

DAVID SOBEL & ARSHAD NAWAZ

SCHOOL OF ENGINEERING AND APPLIED SCIENCE
THE GEORGE WASHINGTON UNIVERSITY
WASHINGTON, D.C. 20006

SEPTEMBER 1972

Reproduced by
NATIONAL TECHNICAL
INFORMATION SERVICE
U S Department of Commerce
Springfield VA 22151

D D C
1973

PREPARED UNDER CONTRACT FOR
MECHANICAL EQUIPMENT BRANCH
NAVAL AIR SYSTEMS COMMAND,
NAVAIR CONTRACT NO. N00019-72-C-0122.

APPROVED FOR PUBLIC RELEASE;
DISTRIBUTION UNLIMITED

ACKNOWLEDGMENT

This work was supported by the Mechanical Equipment Branch of the U. S. Naval Air Systems Command, under contract Number N00019-72-C-0122.

ABSTRACT

This report deals with the design of a Foa Energy Separator for use in a supersonic aircraft, the LTV F-8U Crusader. Calculations are carried out to obtain a range of exit nozzle area ratios compatible with a variety of operating conditions. The effects of variations of the peripheral rotor velocity and discharge pressures on both the hot and cold outputs are analyzed. The potential merit of using a heat exchanger in conjunction with the separator, or of using ram air rather than bleed air, is also discussed.

Area ratios between 0.30 and 0.50 are found to be suitable for all cases. However, in the maximum speed cases the direct use of bleed air does not lead to acceptably low temperatures. The use of a heat exchanger improves performance considerably, as does the use of ram air, although not quite as effectively.

NOMENCLATURE

$\vec{c}$	= fluid particle velocity in F_s
h^o	= specific stagnation enthalpy in F_u
$\dot{m}$	= mass flow rate
p	= static pressure
p^o	= stagnation pressure in F_u
R	= universal gas constant
T	= static temperature
T^o	= stagnation temperature in F_u
u	= particle velocity in F_u
u'	= prerotation velocity
V	= peripheral rotor velocity
α_b/α_a	= ratio of total nozzle exit area on the hot side to total nozzle exit area on the cold side
γ	= ratio of specific heats
δ	= $\cos\theta$ (negative on cold side)
η	= nozzle efficiency
θ	= angle $(\vec{V},-\vec{c})$
κ	= cooling capacity coefficient
μ	= mass flow ratio
ρ	= density

Subscripts

a = cold side

b = hot side

d = discharge condition

i = energy separator inlet flow

o = conditions resulting from isentropic discharge from p_i^o to p_d

INTRODUCTION

Fluid dynamic energy separation is a process in which an initially homogeneous stream of a fluid is separated into two streams at different energy levels. In the Foa Energy Separator this process is cryptosteady, thereby combining the advantages of analytical simplicity in the frame of reference F_s in which the flow field is stationary with the performance advantages of nonsteady flow in the reference frame of application, F_u. A detailed explanation of the principle of the Foa Energy Separator is presented in Reference (1) and will not be repeated here.

This report deals, instead, with the performance of the Foa Energy Separator in a specific application to supersonic aircraft. The data for the F-8U aircraft was selected for performance calculations. This aircraft was manufactured by the LTV Aerospace Corporation and is a refined version of the LTV Crusader. Maximum level flight Mach number is nearly 2.

ANALYSIS

Data presented in Hamilton Standard Report 1034 (12/10/53) provide bleed air temperatures and pressures for the F-8U aircraft at various altitudes and operating modes. The information is presented below and will henceforth be referred to by case number.

I. F-8U Aircraft Data

CASE	ALTITUDE (FT)	OPERATING MODE	BLEED STAGNATION PRESS. (PSI)	BLEED STAGNATION TEMP. (°R)	STANDARD ATMOS. STATIC PRESS (PSI)	STANDARD ATMOS. STATIC TEMP. (
1	0	Max.speed/lvl.	197.1	1275	14.7	518.7
2	0	Loiter	48.6	710	14.7	518.7
3	0	Idle letdown	23.9	555	14.7	518.7
4	10,000	Max.speed/lvl. wings press.	181.9	1279	10.11	483.0
5	10,000	Max.speed/lvl.	183.2	1279	10.11	483.0
6	10,000	Loiter	45.7	750	10.11	483.0
7	10,000	Idle letdown	19.46	585	10.11	483.0
8	23,000	Max.speed/lvl.	141.7	1230	5.95	436.7
9	25,000	Idle letdown	15.8	615	5.45	429.5
10	35,000	Max.speed/lvl. wings press.	124.0	1250	3.46	393.9
11	35,000	Max.speed/lvl.	124.5	1250	3.46	393.9
12	35,000	Loiter	31.6	755	3.46	393.9
13	35,000	Idle letdown	15.9	650	3.46	393.9
14	45,000	Cruise	33.7	985	2.14	390.0
15	51,500	Loiter	25.3	885	1.57	390.0
16	57,500	Max.speed/lvl.	19.2	1040	1.17	390.0
17	57,500	Idle letdown	17.3	800	1.17	390.0

The equations governing the performance of the Foa Energy Separator are presented below. Derivations may be found in References (1) and (2).

The fluid particle velocity resulting from an isentropic discharge is found on both hot and cold sides as:

$$u_o = \sqrt{2h_i^o[1-(p_d/p_i^o)^{(\gamma-1/\gamma)}]} \qquad (1)$$

The total enthalpy change is given on both sides as:

$$h_d^o - h_i^o = V^2\{- \frac{u'}{V} + 1 + \delta[\eta(\frac{u_o^2}{V^2} + 1 - 2\frac{u'}{V})]^{1/2}\} \qquad (2)$$

and thus the temperature increment on each side is

$$T_d^o - T_i^o = \frac{V^2}{6000} \{- \frac{u'}{V} + 1 + \delta[\eta(\frac{u_o^2}{V^2} + 1 - 2\frac{u'}{V})]^{1/2}\}. \qquad (3)$$

For example, on the cold side,

$$T_i^o - T_a^o = \frac{V_a^2}{6000} \{\frac{u'_a}{V} - 1 - \delta_a[\eta_a(\frac{u_{oa}^2}{V^2} + 1 - 2\frac{u'_a}{V})]^{1/2}\}.$$

By definition the mass flow ratio is

$$\mu = \dot{m}_b/\dot{m}_a = (h_i^o - h_a^o)/(h_b^o - h_i^o) \qquad (4)$$

also the cooling capacity coefficient is

$$\kappa = \dot{m}_a(h_i^o - h_a^o)/\dot{m}_i V_a^2 \qquad (5)$$

The above equations apply to both the internal and external separation configurations of the Foa Energy Separator. As this report deals with the design of an internal separation device, where the governing design parameter is the nozzle area ratio a_b/a_a, the following relations become essential [Ref. 2]:

On both sides the fluid particle velocity c, in F_s, and the density ρ, can be found as;

$$c = \sqrt{\eta(V^2 - 2u'V + u_o^2)} \qquad (6)$$

and

$$\rho = \rho_i^o \frac{p_d/p_i^o}{1-\eta[1-(p_d/p_i^o)^{\gamma-1/\gamma}] + (1-\eta)\frac{V^2}{2h_i^o}(1-2\frac{u'}{V})} \tag{7}$$

ρ_i^o can be determined by the perfect gas law as

$$\rho_i^o = p_i^o/RT_i^o$$

and the mass flow ratio μ, can be more conveniently written as

$$\mu = \frac{u_a'+c_a\delta-V}{V-u_b'+c_b\delta} \tag{8}$$

where c is found from Equation (6).

Finally, the nozzle area ratio α_b/α_a, is

$$\alpha_b/\alpha_a = \mu\frac{c_a}{c_b}\frac{\rho_a}{\rho_b} \tag{9}$$

where c, ρ, and μ are found from Equations (6), (7) and (8) respectively.

For design calculations the following was assumed in this analysis: nozzle efficiencies on the cold side of 0.90 (η_a=0.90) and on the hot side of 0.80 (η_b=0.80) and nozzle inclinations of 18° (δ=cosθ=δ_b=-δ_a=0.95). Prerotation velocities on the hot and cold sides were assumed to be zero (u_a'=u_b'=0.0) and it was further assumed that the rotor peripheral velocities on the hot and cold sides were equal (V_a=V_b=V).

The relations between rotor peripheral velocity, nozzle area ratio and stagnation temperature drop on the cold side

are illustrated by the group of graphs labelled "A" in the appendix. The graphs represent sea level conditions (Cases 1, 2 and 3) and were constructed using Equations (9) and (3). For each case, one graph gives the nozzle area ratio required to produce a given peripheral velocity and the other gives the stagnation temperature drop obtained at that velocity. It was assumed for these calculations that the discharge pressures on the hot and cold side were equal to the standard atmospheric pressure. Due to structural limitations, the maximum peripheral velocity considered was 1,000 feet per second.

It can be seen from Case 3 (Graph A3b) that the temperature drop is not necessarily a maximum when the rotor peripheral velocity is. This can be derived as follows:

From Equation (3), and for the stated conditions,

$$\Delta T_a^o = -\frac{V^2}{6000} + (.15\times10^{-3})(u_{oa}^2 V^2 + V^4)^{1/2}$$

ΔT_a^o is maximum for

$$\frac{d(\Delta T_a^o)}{dV} = -\frac{V}{3000} + (.15\times10^{-3})(u_{oa}^2 V + 2V^3)/(u_{oa}^2 V^2 + V^4)^{1/2}$$

$$= 0$$

i.e., for

$$V = 0.8087 u_{oa}$$

This result shows that, for maximum cooling, the rotor speed may have to vary from case to case. This can be

accomplished in any one of three ways. First, as can be seen from the graphs in Appendix "A" (A1a, A2a, A3a), the velocity can be varied by altering the area ratio, maintaining atmospheric discharge pressures. However, it would be impracticable to vary the nozzle area ratio once set.

On the other hand, with a given area ratio, the velocity will vary automatically from case to case due to changes in inlet and exit pressures, as specified in Table I. This fails, however, to provide an area ratio suitable for all cases. For instance, an area ratio of 0.50 would produce a very low peripheral velocity in Case 3, but would produce a velocity in excess of the 1000 fps limit in Case 1. In fact, there is no area ratio compatible with both cases. Thus, this method is also inadequate for design purposes. The third possibility is the variation of either the hot or cold side discharge pressure.

The effect of the variation of the discharge pressure on the cold side was the first possibility considered. Graphs "D" of the appendix illustrate the effect of the variation of the cold side discharge pressure on both the nozzle area ratio required for a given peripheral velocity and the cold output temperature drop. It was assumed for these calculations that the hot side discharge pressure was atmospheric. As previously, all seventeen cases were analyzed, but since the first three cases were found to be representative, they are the only ones presented here. It can be seen from these

graphs that a range of compatible area ratios does exist. It is interesting to note that with any given area ratio, the same rotor speed can be achieved, everything else being equal, with two different discharge pressures on the cold side. These correspond to supersonic and subsonic discharge. All discharge pressures lower than that corresponding to the minimum area ratio obtainable imply supersonic discharge; higher pressures, subsonic. It can be seen from the graphs for cold discharge pressure vs. cold temperature drop of section "D" of the appendix that it is advantageous to use a supersonic discharge. For instance, in Case 1 with rotor peripheral velocity equal to 800 fps (Graphs $D1a_1$, $D1b_1$), and an area ratio of 0.50, the supersonic discharge corresponding to a discharge pressure of 8.5 psi produces a temperature drop of 268° R, while the subsonic discharge corresponding to a discharge pressure of 137 psi, produces a temperature drop of only 70° R. The effect of varying the cold discharge pressure on the mass flow ratio and the cooling capacity coefficient are displayed in section "E" of the appendix. It is seen that lowering the cold side discharge pressure increases both the mass flow ratio and the cooling capacity coefficient.

The effect next considered was that of the variation of the hot side discharge pressure. Graphs "B" of the appendix illustrate the manner in which the required nozzle area ratio varies with the hot side discharge pressure for a given rotor velocity. As in the case of the cold side discharge pressure

variation, two solutions are present here, the lower hot side discharge pressure corresponding to supersonic discharge; higher pressure, subsonic. Unlike the case of the cold side discharge pressure variation, supersonic and subsonic hot side discharge pressures produce identical cold side temperature drops. This can be seen from Equation (3), where for a given rotor velocity the hot side discharge pressure has no effect on the cold side temperature drop. It does however, effect other parameters of importance. Graphs "C" of the appendix illustrate the relation between the hot side discharge pressure and both the mass flow ratio and cooling capacity coefficient as computed from Equations (4) and (5), respectively. As can be seen, decreasing the discharge pressure below atmospheric has the effect of decreasing the mass flow ratio and increasing the cooling capacity coefficient.

A comparison of the cold side temperature drop obtainable from variation of the hot or cold side discharge pressure shows that latter to be more effective. For any given area ratio and rotor peripheral velocity, there is a distinct advantage in controlling the cold side discharge pressure. For instance, in Case 1, with a fixed rotor velocity of 1000 fps and atmospheric discharge on the cold side, the cold side temperature drop remains 284° R regardless of the value of the hot side discharge pressure. On the other hand, with atmospheric back pressure on the hot side, the cold side temperature drop can reach as high as 360° R (Graph $D1b_3$)

by control of the cold side back pressure.

Controlling the cold side discharge pressure (this being more effective than controlling the hot side discharge pressure), a nozzle area ratio suitable for all seventeen cases was sought. Calculations were done as follows: A rotor peripheral velocity, say 1000 fps, was chosen. Using Equations (9) and (3) the nozzle area ratio and the cold side temperature drop respectively, were calculated for various cold side discharge pressures, hot side discharge pressure being atmospheric. The cold side discharge pressure was given a lower limit of one-third atmospheric pressure. This procedure was repeated for several velocities between 600 fps and 1000 fps, so that an optimal combination of the area ratio, the cold side discharge pressure and the rotor velocity could be obtained. From these calculations an area ratio could be chosen and the corresponding cold side temperature drop, discharge pressure and rotor velocity were available. The following tables show the results for nozzle area rations of 0.30, 0.40, and 0.50. Area ratios below 0.30 or above 0.50 were not compatible with all cases.

It is obvious from these tables that there are several cases, in particular those which correspond to maximum speed conditions (Cases 1, 4, 8, 10, and 16), whose discharge temperatures are too high to provide adequate cooling. Two possibilities were investigated to remedy this situation.

The first possible remedy is directing the bleed air

II. Performance Calculations Using Bleed Air

$$\alpha_b/\alpha_a = 0.30$$

Case	V(fps)	p_{da}(psi)	T_a^o(°R)	μ	κ
1	1000	5.0	940	.558	1.27
2	800	5.0	556	.503	.961
3	800	6.0	460	.386	.641
4	1000	3.2	939	.568	1.32
5	same as (4)				
6	900	4.0	573	.455	.901
7	800	4.5	480	.365	.684
8	1000	2.0	890	.558	1.31
9	900	4.0	508	.310	.606
10	1000	1.1	894	.567	1.36
11	same as (10)				
12	1000	1.7	550	.418	.868
13	1000	2.5	510	.672	.643
14	1000	0.8	707	.503	1.11
15	1000	0.6	627	.480	1.04
16	1000	0.4	747	.519	1.16
17	1000	0.5	566	.452	.967

$$\alpha_b/\alpha_a = 0.40$$

Case	V(fps)	p_{da}(psi)	T_a^o(°R)	μ	κ
1	1000	7.5	960	.528	1.23
2	600	5.0	580	.640	1.32
3	600	4.0	559	.628	.995
4	1000	5.0	951	.541	1.28
5	same as (4)				
6	700	5.0	603	.541	1.16
7	600	3.5	408	.545	1.02
8	1000	3.0	902	.538	1.28
9	600	2.5	509	.557	1.13
10	1000	1.7	905	.549	1.34
11	same as (10)				
12	1000	3.0	572	.374	.801
13	700	2.0	522	.492	1.05
14	1000	1.3	723	.474	1.07
15	1000	1.0	643	.451	1.00
16	1000	0.7	767	.487	1.11
17	1000	0.9	583	.415	.919

II. Performance Calculations Using Bleed Air (Continued)

$$\alpha_b/\alpha_a = 0.50$$

Case	V(fps)	p_{da}(psi)	T_a^o(°R)	μ	κ
1	1000	11.5	979	.501	1.19
2	600	14.7	618	.451	1.05
3	500	4.5	472	.713	1.67
4	1000	7.5	967	.511	1.24
5	same as (4)				
6	600	6.5	625	.519	1.36
7	500	4.0	500	.663	1.21
8	1000	4.5	915	.515	1.24
9	500	3.0	526	.610	1.33
10	1000	2.5	920	.531	1.31
11	same as (10)				
12	900	4.0	592	.386	.87
13	600	2.8	543	.511	1.19
14	1000	2.0	739	.445	1.02
15	1000	1.6	660	.419	.95
16	1000	1.0	779	.463	1.07
17	1000	1.3	598	.389	.87

through a heat exchanger before entering the energy separator. For simplicity, a heat exchanger effectiveness of 1.0 was chosen: thus, the outlet temperature of the bleed air would be equal to the stagnation atmospheric temperature relative to the aircraft (this stagnation temperature is found as $T^{o}_{ATM} = T_{ATM}(1 + \frac{\gamma-1}{2} M^{2}_{F-8u})$). Calculations were done using standard atmospheric data and a maximum speed performance of Mach 2. The results of these calculations are displayed in the tables below for nozzle area ratios of 0.30, 0.40 and 0.50.

III. Performance Using Bleed Air With Heat Exchanger

$\alpha_b/\alpha_a = 0.30$

Case	V(fps)	T^{o}_{i}(°R)	p_{da}(psi)	T^{o}_{a}(°R)	μ	κ
1	1000	934	5.7	673	.487	1.06
4	1000	869	4.5	613	.470	1.03
8	1000	787	2.5	543	.459	1.00
10	1000	709	1.5	476	.444	.97
16	1000	702	0.6	487	.418	.85

$\alpha_b/\alpha_a = 0.40$

Case	V(fps)	T^{o}_{i}(°R)	p_{da}(psi)	T^{o}_{a}(°R)	μ	κ
1	1000	934	9.5	690	.455	1.01
4	1000	869	6.5	628	.450	1.00
8	1000	787	4.0	555	.436	.97
10	1000	709	2.4	485	.425	.94
16	1000	702	0.9	504	.395	.85

III. Performance Using Bleed Air With Heat Exchanger (Cont.)

$\alpha_b/\alpha_a = 0.50$

Case	V(fps)	T_i^o(°R)	p_{da}(psi)	T_a^o(°R)	μ	κ
1	1000	934	14.7	707	.422	.96
4	1000	869	9.9	642	.423	.96
8	1000	787	5.9	566	.415	.93
10	1000	709	3.4	494	.409	.92
16	1000	702	1.5	520	.363	.80

It is easily seen that the heat exchanger provides significantly increased performance. It also allows the use of slightly higher discharge pressures which would be more easily obtainable than those required by the direct use of bleed air.

The possibility of using ram air rather than bleed air was also considered. Again, assumptions were a maximum flight Mach number of 2 and standard atmospheric conditions. The atmospheric stagnation pressure and temperature relative to the aircraft are given by

$$p_o^o = p_{ATM}(1 + \frac{\gamma-1}{2} M_{F-8u}^2)^{\gamma-1/\gamma}$$

and

$$T_o^o = T_{ATM}(1 + \frac{\gamma-1}{2} M_{F-8u}^2)$$

For calculation purposes a Kantrowitz-Donaldson air intake designed for a free stream Mach number of 2 was assumed. At Mach 2 the corresponding stagnation pressure ratio is approximately 0.85 (p_i^o/p_o^o=0.85). Since the flow can be assumed to be adiabatic and isoenergetic, T_o^o=T_i^o. The calculation pro-

cedure used was similar to that for bleed air, the results are displayed below.

IV. Performance Using Ram Air

$\alpha_b/\alpha_a = 0.30$

Case	V(fps)	T_i^o(°R)	p_{da}(psi)	T_a^o(°R)	μ	κ
1	1000	934	6.0	699	.466	.96
4	1000	869	4.4	649	.446	.92
8	1000	787	2.9	586	.416	.85
10	1000	709	1.9	529	.385	.78
16	1000	702	0.6	520	.388	.79

$\alpha_b/\alpha_a = 0.40$

Case	V(fps)	T_i^o(°R)	p_{da}(psi)	T_a^o(°R)	μ	κ
1	1000	934	11.4	729	.407	.88
4	1000	869	8.7	680	.383	.82
8	1000	787	6.0	620	.347	.74
10	1000	709	4.4	568	.301	.65
16	1000	702	1.6	566	.291	.63

These figures show that while the cold side output temperatures using ram air are significantly lower than those corresponding to the direct use of bleed air (Table II), they are slightly higher than those obtained using the bleed air-heat exchanger combination (Table III).

The use of a heat exchanger or ram air is highly advisable for aircraft with performance similar to that of the F-8U (Mach 2). However, as the Mach number is increased the performance of the heat exchanger is decreased as the stagnation

temperature rises to the level of the bleed temperature. For example, in Case 1 the stagnation temperature of atmospheric air (relative to the aircraft) is equal to the bleed temperature of 1275° R at Mach 2.7. Thus at Mach 2.7 the heat exchanger would serve no advantage as no heat could be extracted from the bleed air. Similarly, the temperature of the ram air would equal that of the bleed air and would have the added disadvantage of a low inlet pressure.

CONCLUSIONS

The choice of one particular nozzle area ratio is difficult, if not impossible, to make without further information regarding the specific requirements of performance. For any given case and rotor peripheral velocity, lower area ratios provide lower output temperatures, however, they require greater reductions of the cold side discharge pressure than do the larger area ratios. Also, smaller area ratios reduce the mass flow on the cold side.

The direct use of bleed air as energy separator input produces adequate cooling in most cases, but not at maximum aircraft speed. A comparison of Table IV with Table II shows that significantly lower output temperatures can be realized using ram air rather than bleed air directly. On the other hand, the bleed air-heat exchanger combination (Table III) exhibits slightly lower output temperatures than those of ram air. However, elimination of the bulky heat exchanger would probably more than compensate for the slightly higher temperatures obtained using ram air. Cases 1 and 4 still exhibit temperatures higher than desired, even when utilizing ram air or a heat exchanger. Among the alternative solutions that remain to be investigated are the following; (a) lower pressure bleed off, (b) staging, (c) looping and (d) prerotation.

Utilizing the bleed off from an intermediate, rather than the final, stage of the engine would provide a lower

pressure and lower temperature energy separator input. A compromise would have to be made between the loss in performance due to the lower pressure input and the advantage of the lower temperature input. The simplest staging configuration would use the cold output of a first energy separator as the input to a second. The third and most attractive alternative is looping. One possible looping configuration would be to use the air leaving the cooled chamber to cool the energy separator input (ram or bleed air). As the air leaving the chamber is still relatively cool, the heat exchanger required to significantly lower the separator input temperature, would be relatively small. The potential merit of prerotation has been discussed in Reference [2].

REFERENCES

1. Foa, J. V., "Energy Separator," Rensselaer Polytechnic Institute Tech. Report, TR AE 6401, January 1964.

2. Foa, J. V., "Performance of the Cryptosteady Flow Energy Separator," The George Washington University Report, TR-ES-722, July 1972.

APPENDIX SECTION A: BASIC PERFORMANCE CALCULATIONS

Cases 1, 2 and 3

Nozzle Area Ratio vs. Peripheral Rotor Velocity

Cold Side Temperature Difference vs. Peripheral Rotor Velocity

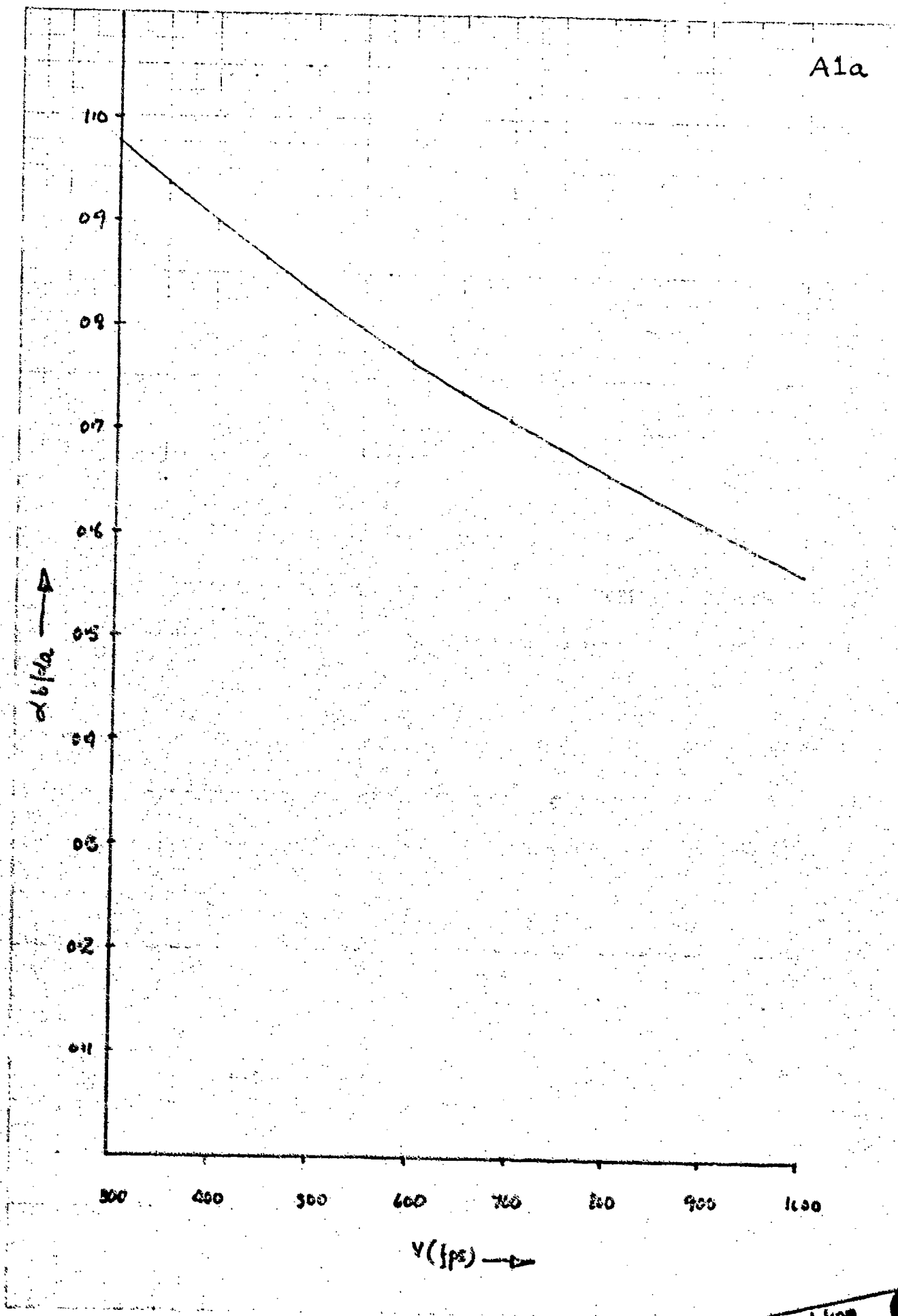

Reproduced from best available copy.

A1b

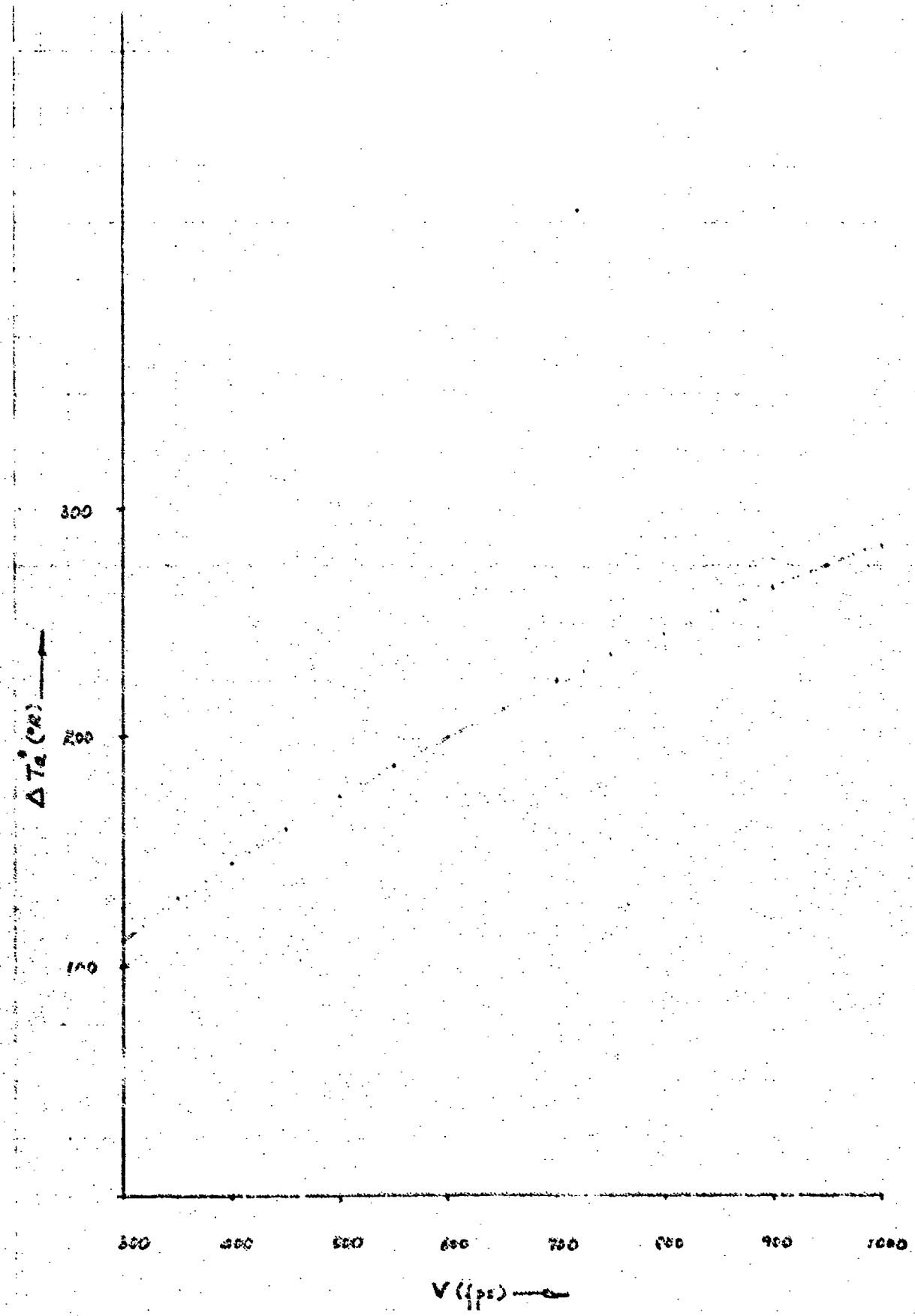

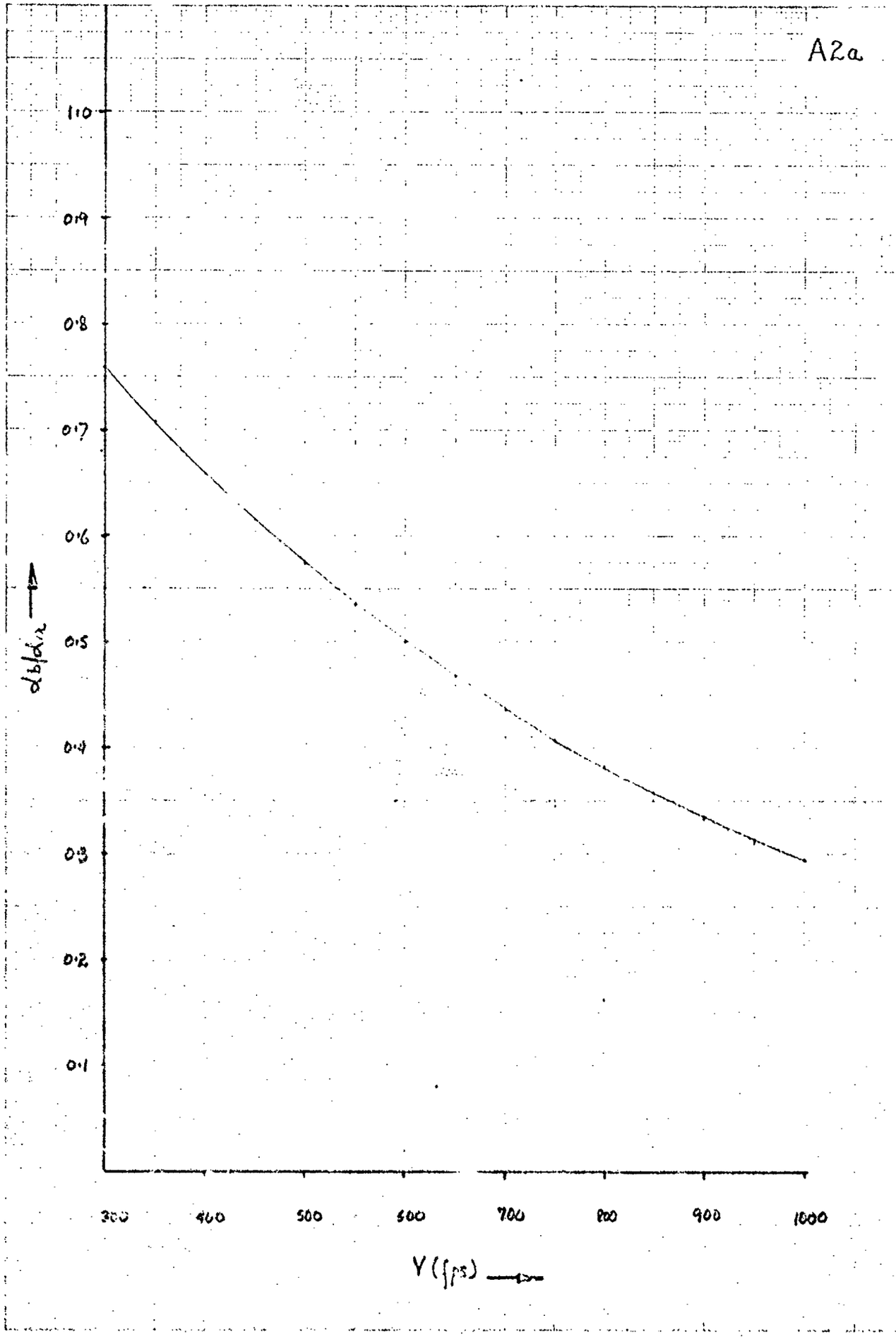
A2a
1.0
0.9
0.8
0.7
0.6
0.5
0.4
0.3
0.2
0.1
$\alpha b/\alpha_2$
300
400
500
600
700
800
900
1000
V (fps)

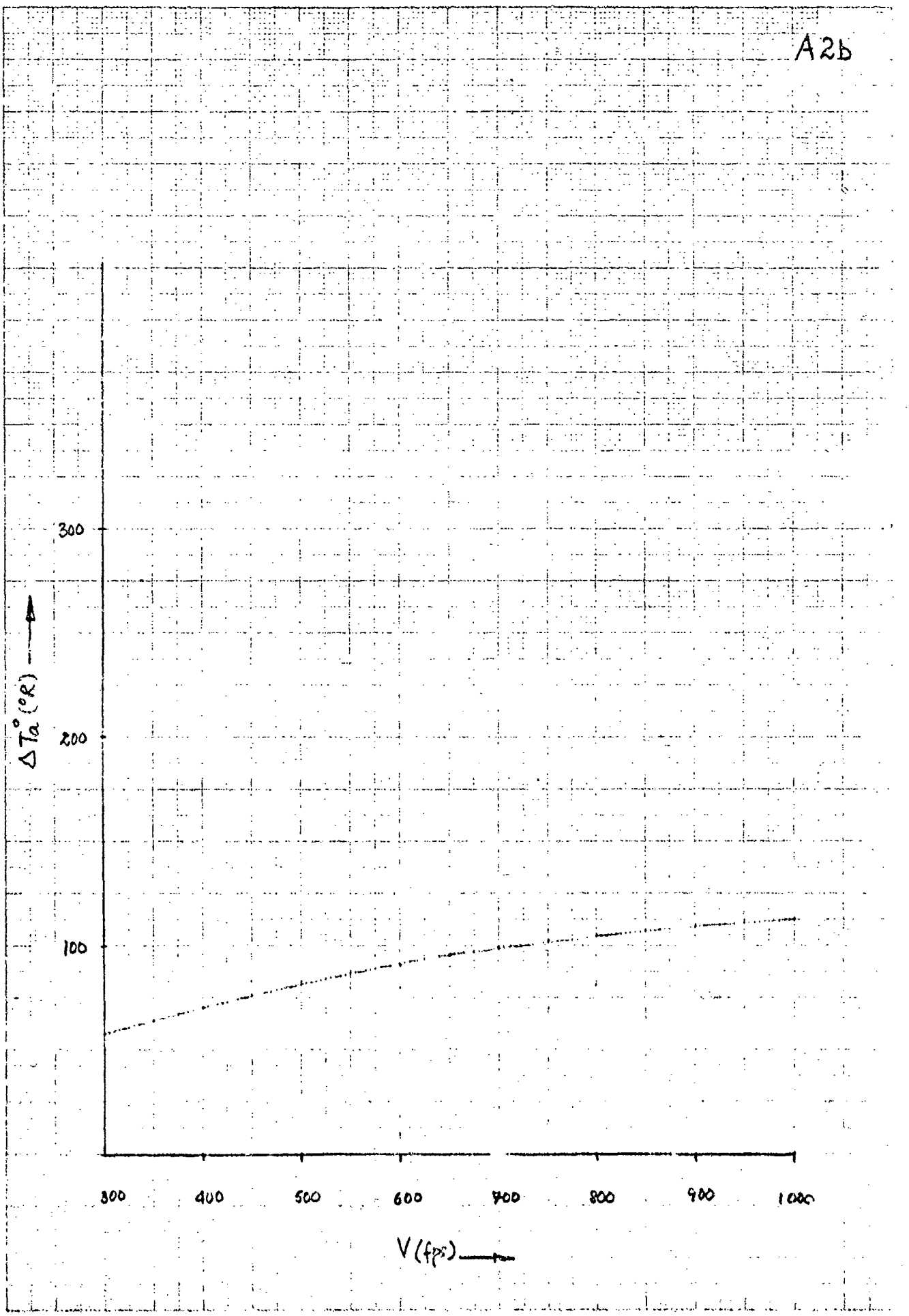

Millimeters to the Centimeter

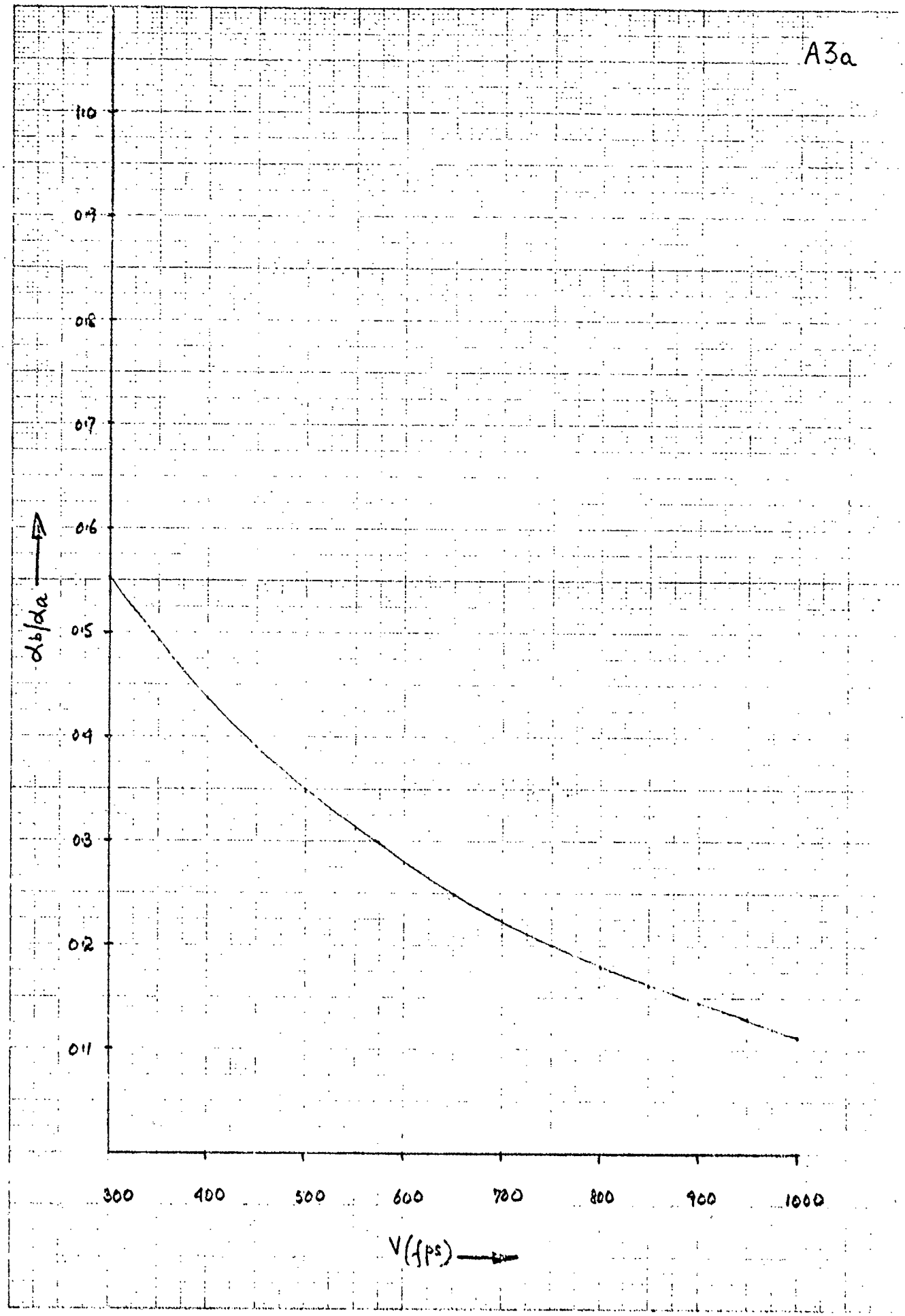

Millimeters to the Centimeter

NATIONAL
12 188

A3b

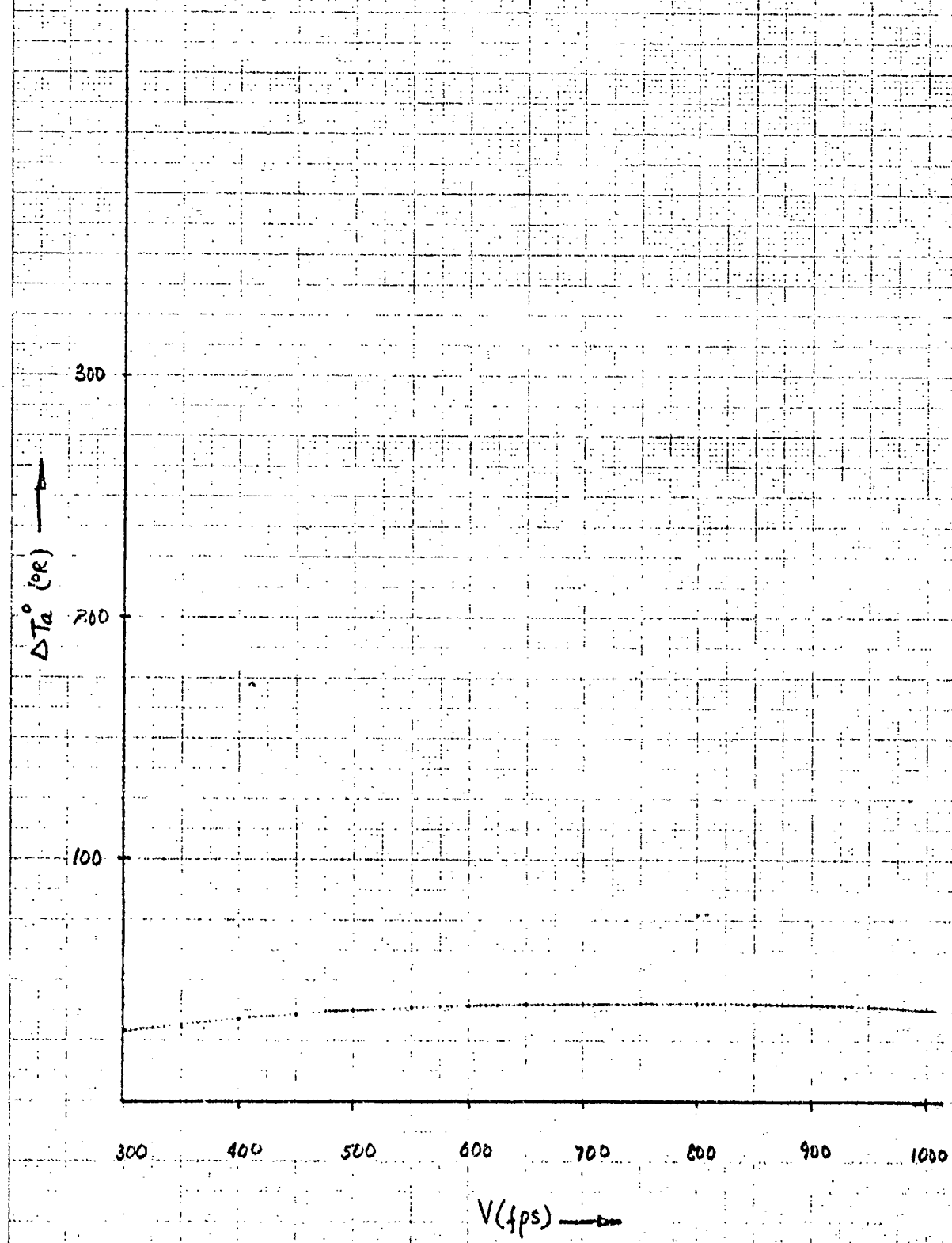

Millimeters to the Centimeter

APPENDIX SECTION B: VARIATION OF p_{db}

Cases 1, 2 and 3 (V=1000 fps)

Nozzle Area Ratio vs. Hot Discharge Pressure

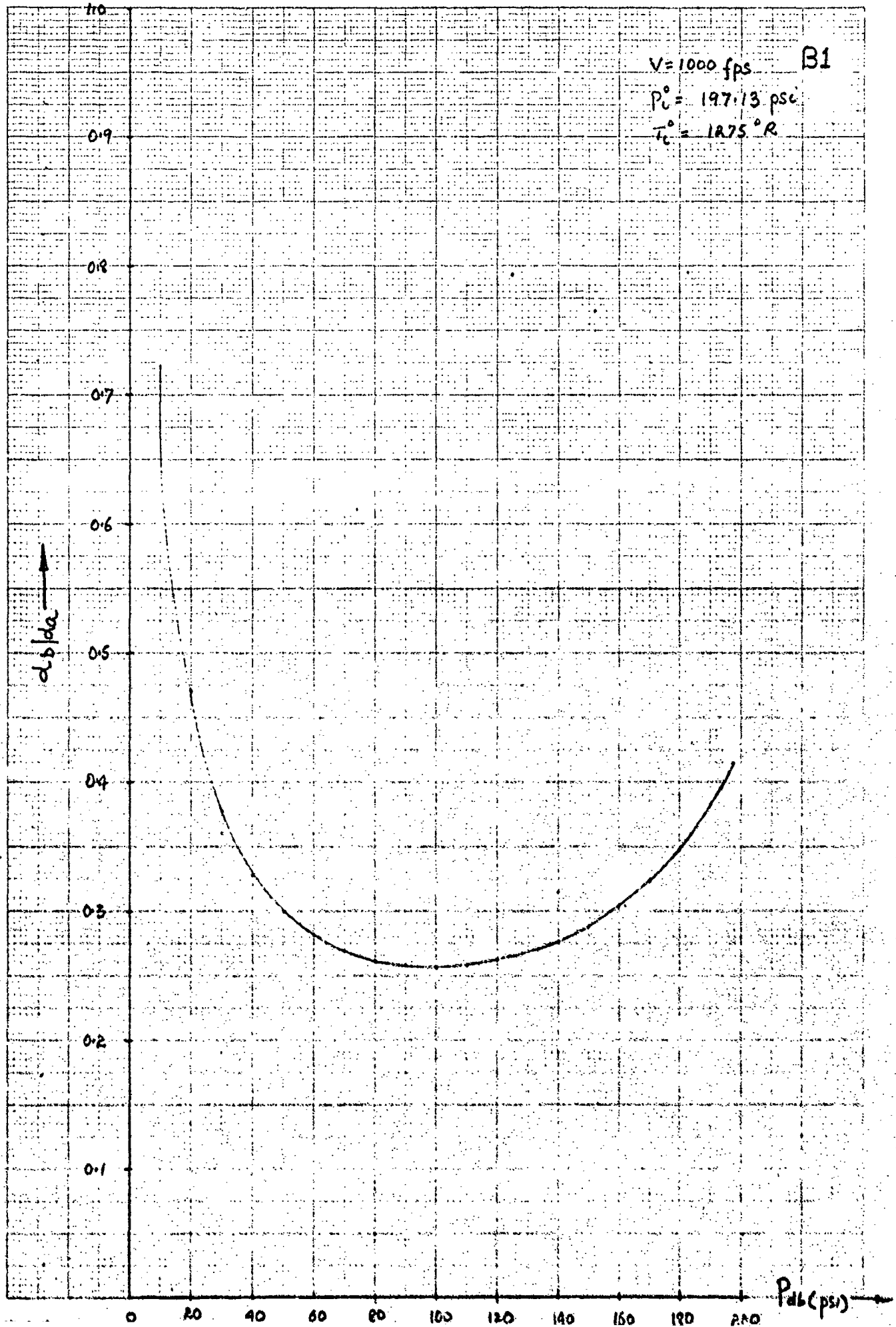
V = 1000 fps
B1
P_c^o = 197.13 psi
T_c^o = 1275 °R
1.0
0.9
0.8
0.7
0.6
0.5
0.4
0.3
0.2
0.1
d_b/d_a
0
20
40
60
80
100
120
140
160
180
200
P_{db} (psi)

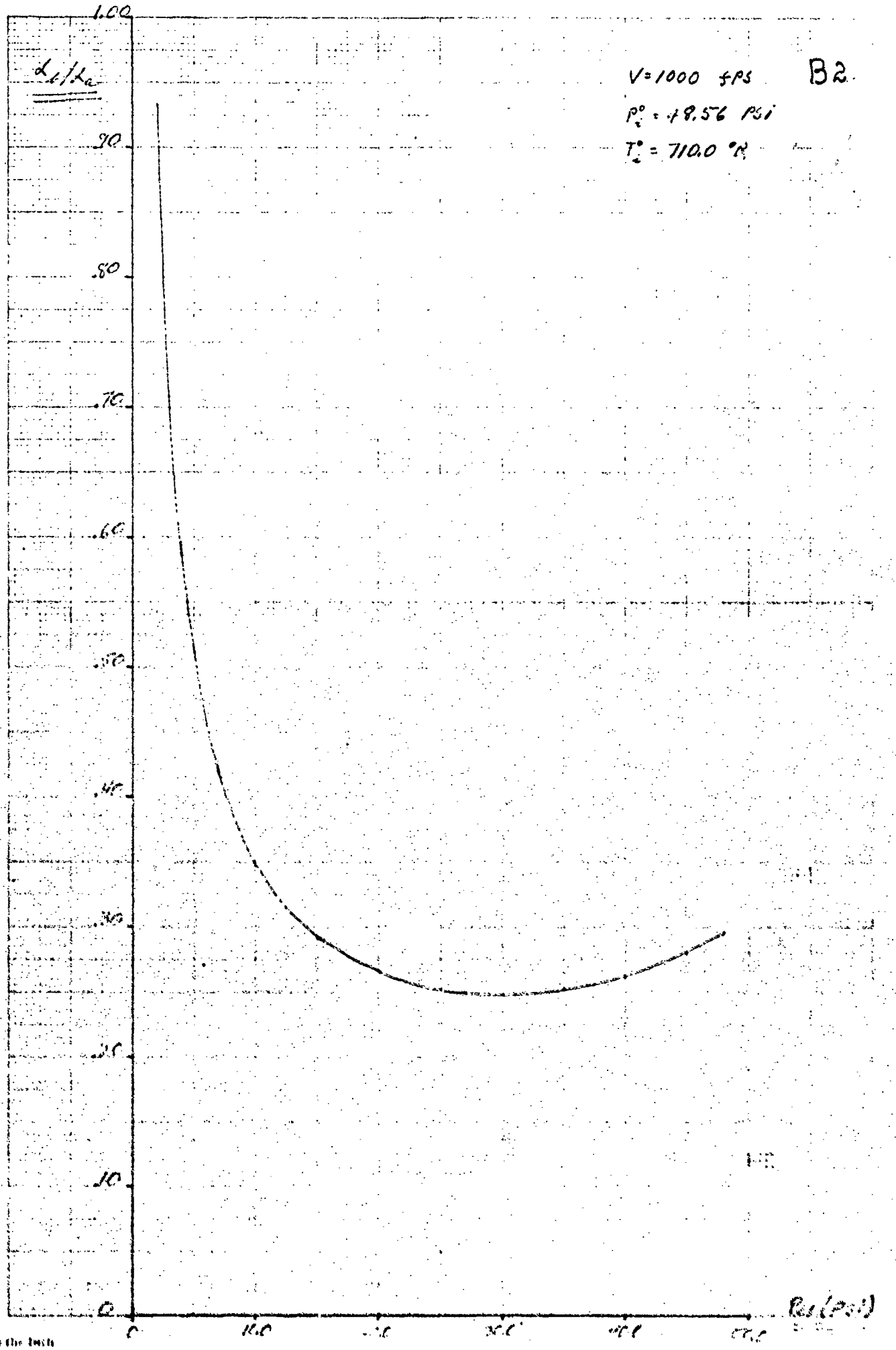

α_b/α_a
V=1000 fps
B2
P_i^o = 48.56 psi
T_i^o = 710.0 °R
1.00
.90
.80
.70
.60
.50
.40
.30
.20
.10
0
0
10.0
20.0
30.0
40.0
50.0
Pa (psi)

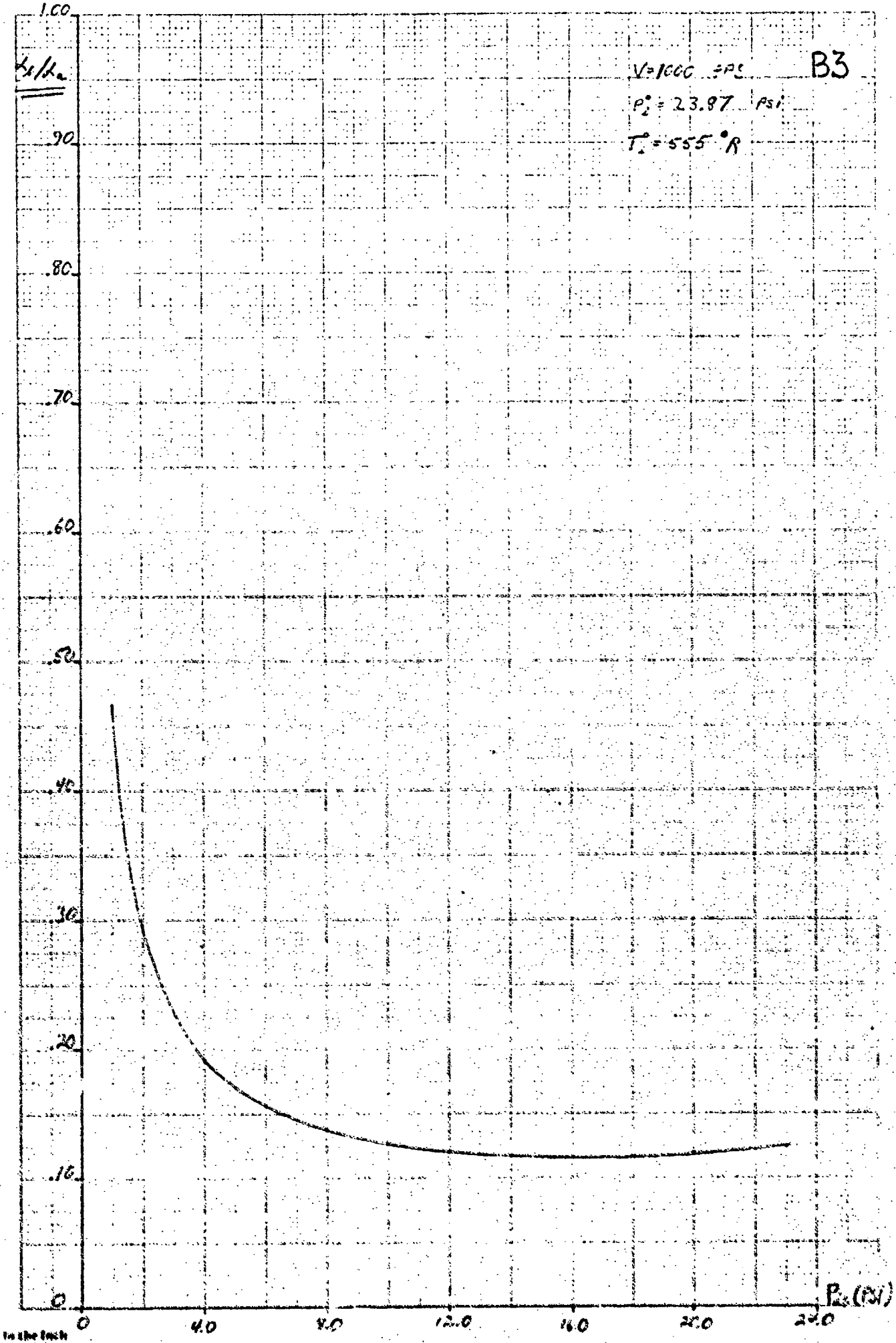
B3
V=1000 FPS
$P_2^* = 23.87$ psi
$T_2^* = 555$ °R
h_1/h_2
1.00
.90
.80
.70
.60
.50
.40
.30
.20
.10
0
0
4.0
8.0
12.0
16.0
20.0
24.0
P_2 (PSI)

APPENDIX SECTION C: EFFECT OF VARIATION OF p_{db} ON μ AND κ

Case 1 (V=800, 1000 fps)

Mass Flow Ratio vs. Hot Discharge Pressure

Cooling Capacity Coefficient vs. Hot Discharge Pressure

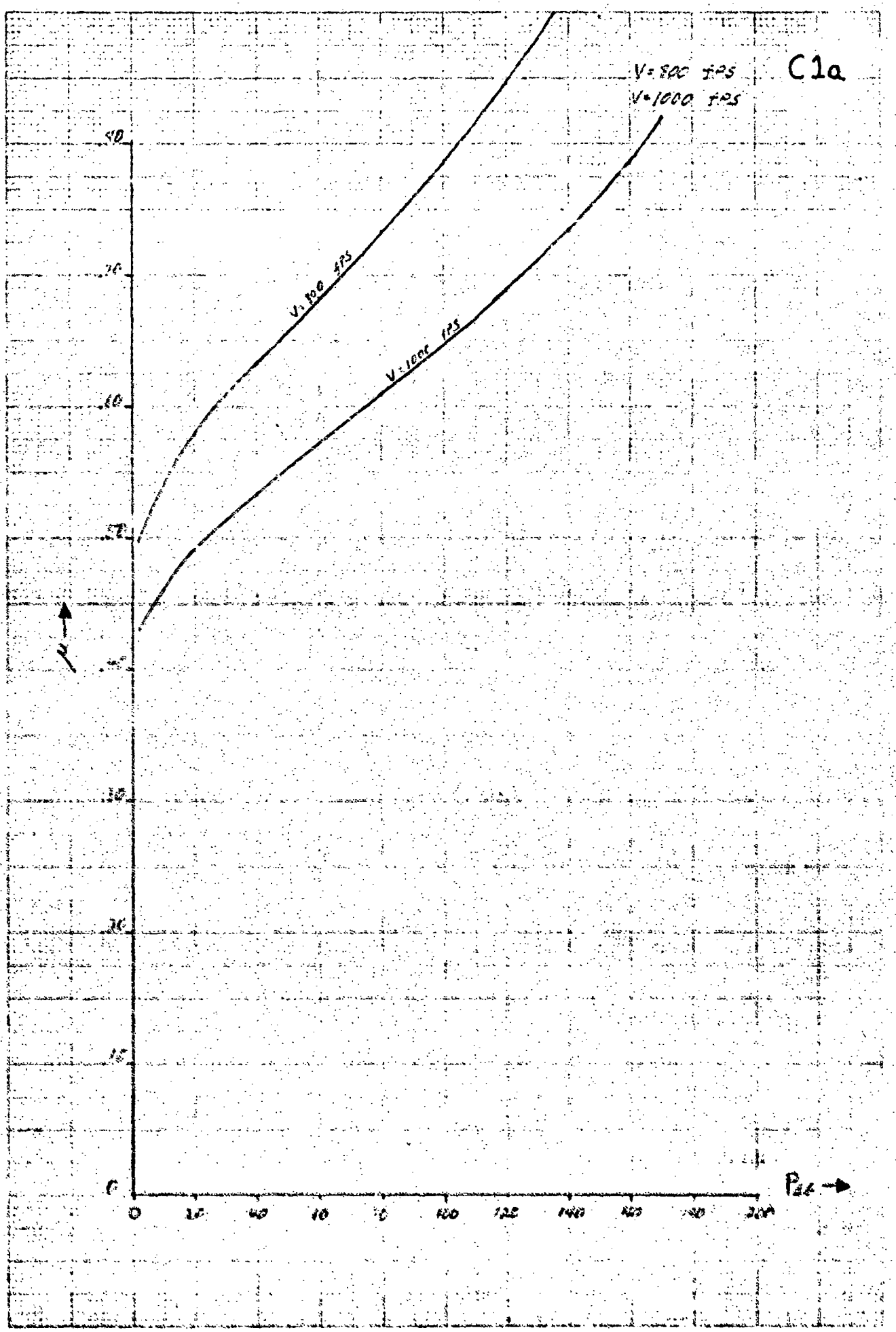
C1a
V=800 fps
V=1000 fps
V=800 fps
V=1000 fps
μ
0
10
20
30
40
50
60
70
80
0
20
40
60
80
100
120
140
160
180
200
P_{dB}

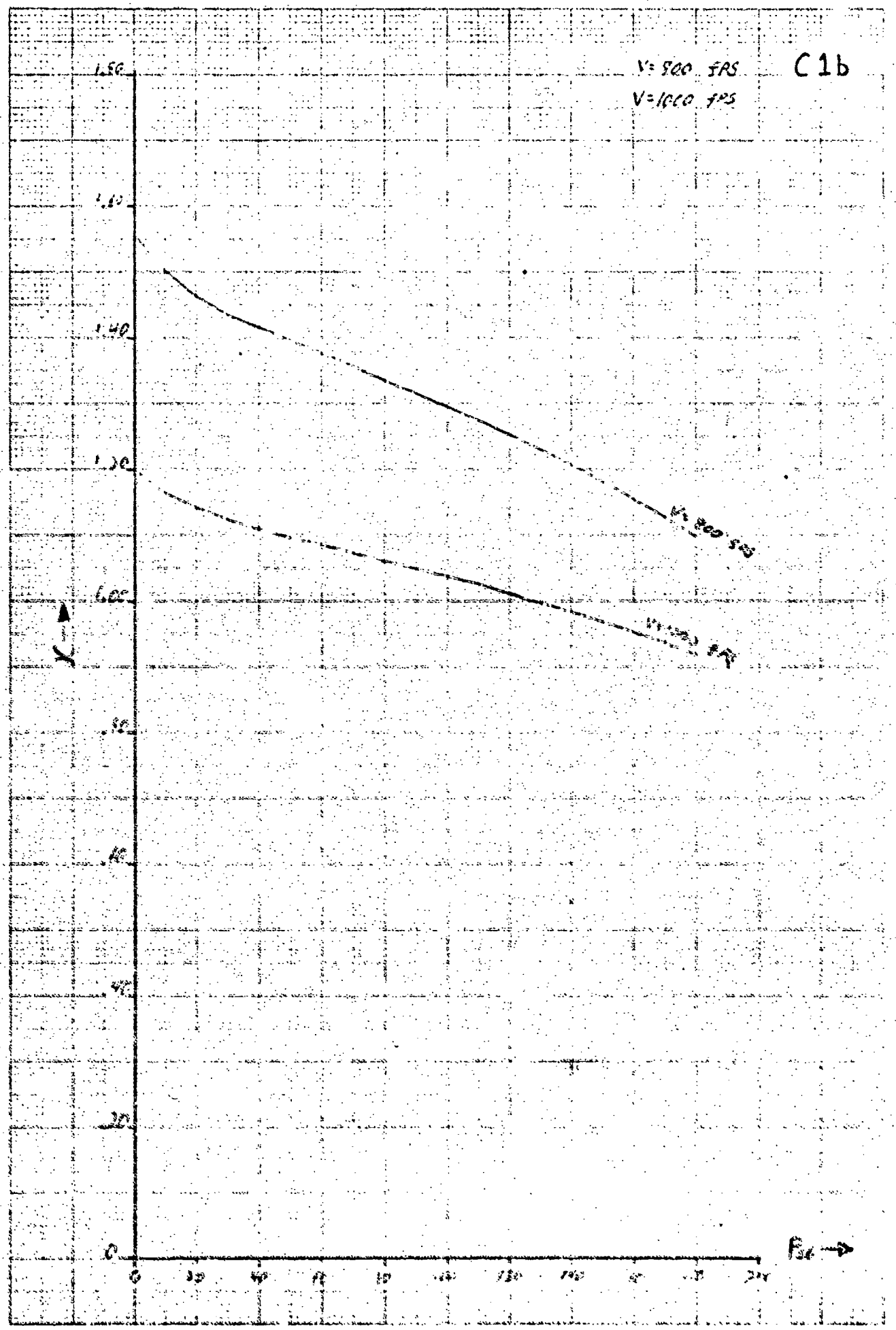
V= 800 fps
V=1000 fps
C1b
1.50
1.40
1.30
1.00
.80
.60
.40
.20
0
X
0
20
40
60
80
100
120
140
160
180
200
Pa

APPENDIX SECTION D: VARIATION OF p_{da}

Cases 1, 2 and 3 (V=800, 900 and 1000 fps)

Nozzle Area Ratio vs. Cold Discharge Pressure

Cold Temperature Difference vs. Cold Discharge Pressure

L_e/L_a
V=800 fps
D1a1
P_a^o=197.13 psi
T_a^o=1275 °R
1.00
.90
.80
.70
.60
.50
.40
.30
.20
.10
0
P_{da}

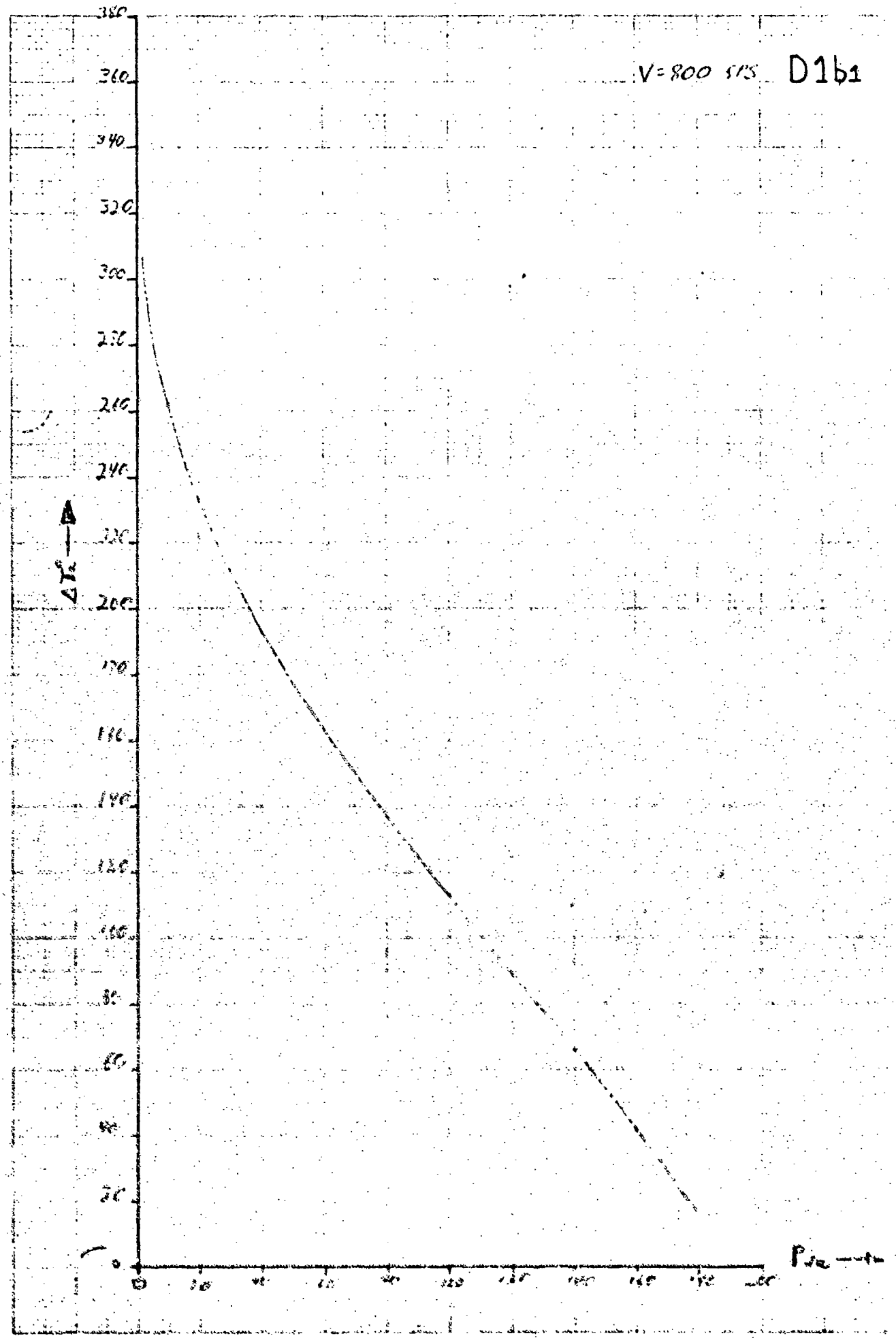
V=800 fps
D1b1
380
360
340
320
300
280
260
240
220
200
180
160
140
120
100
80
60
40
20
0
0
20
40
60
80
100
120
140
160
180
200

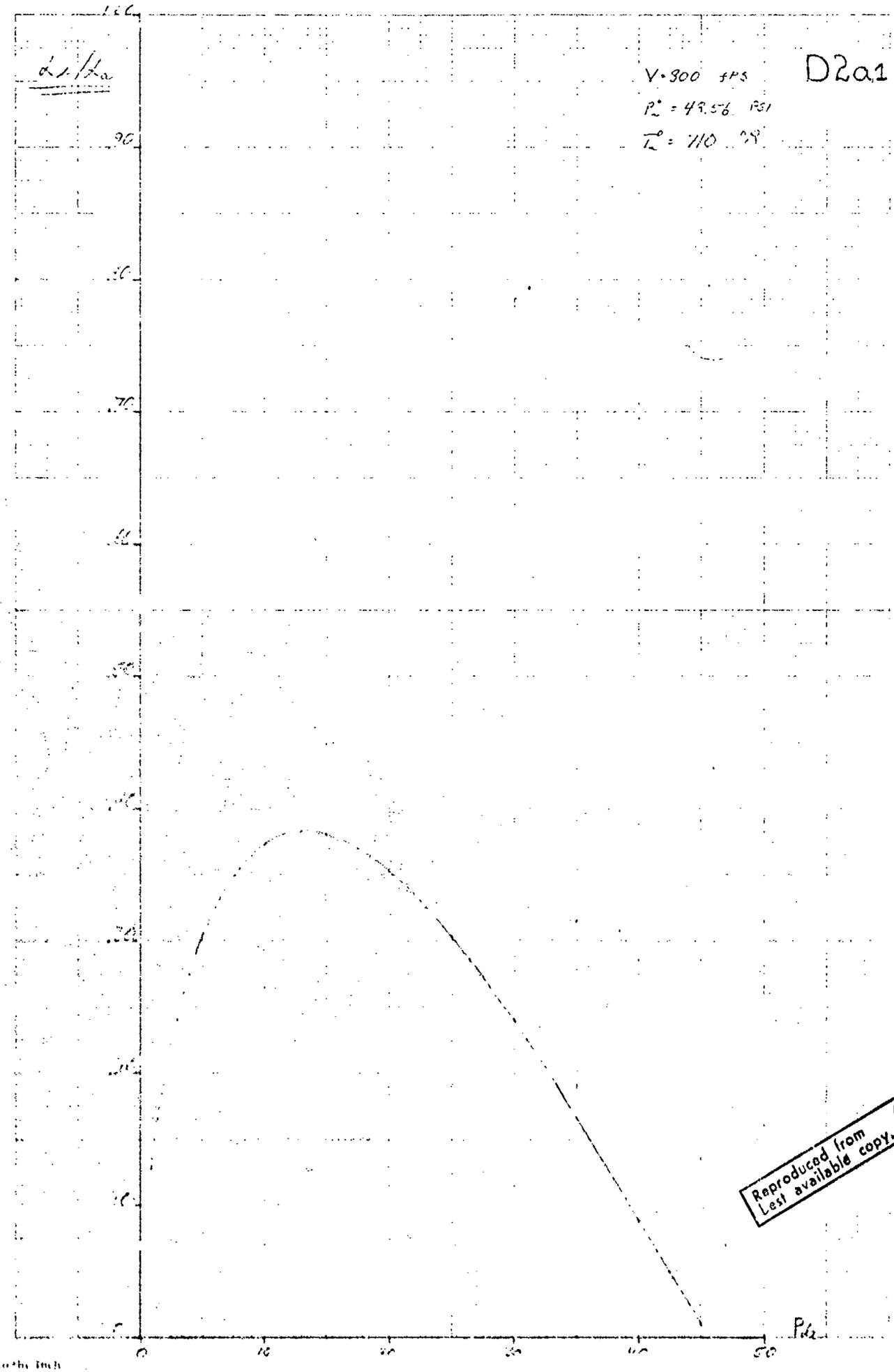

Reproduced from best available copy.

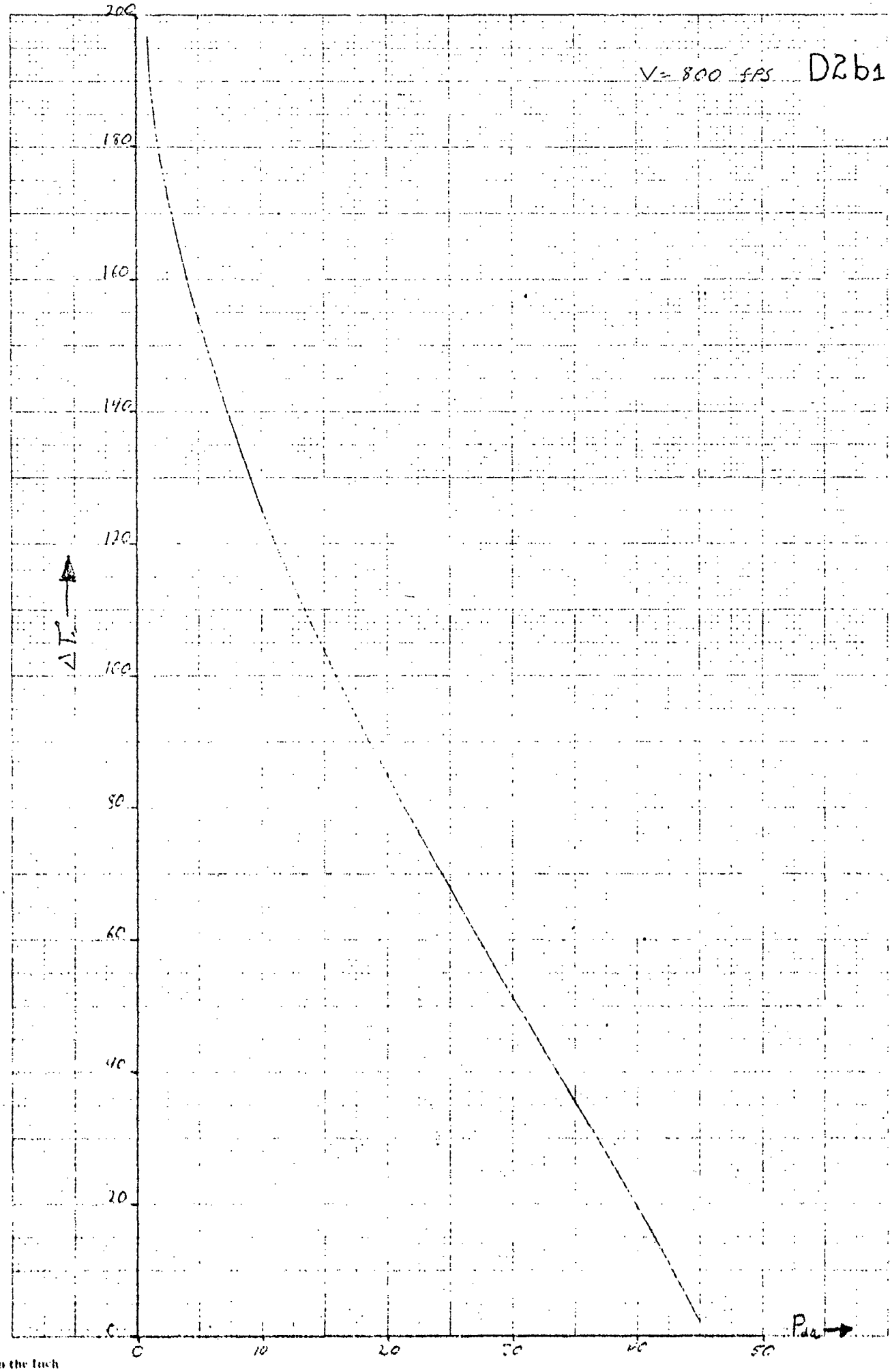

* Squares to the Inch

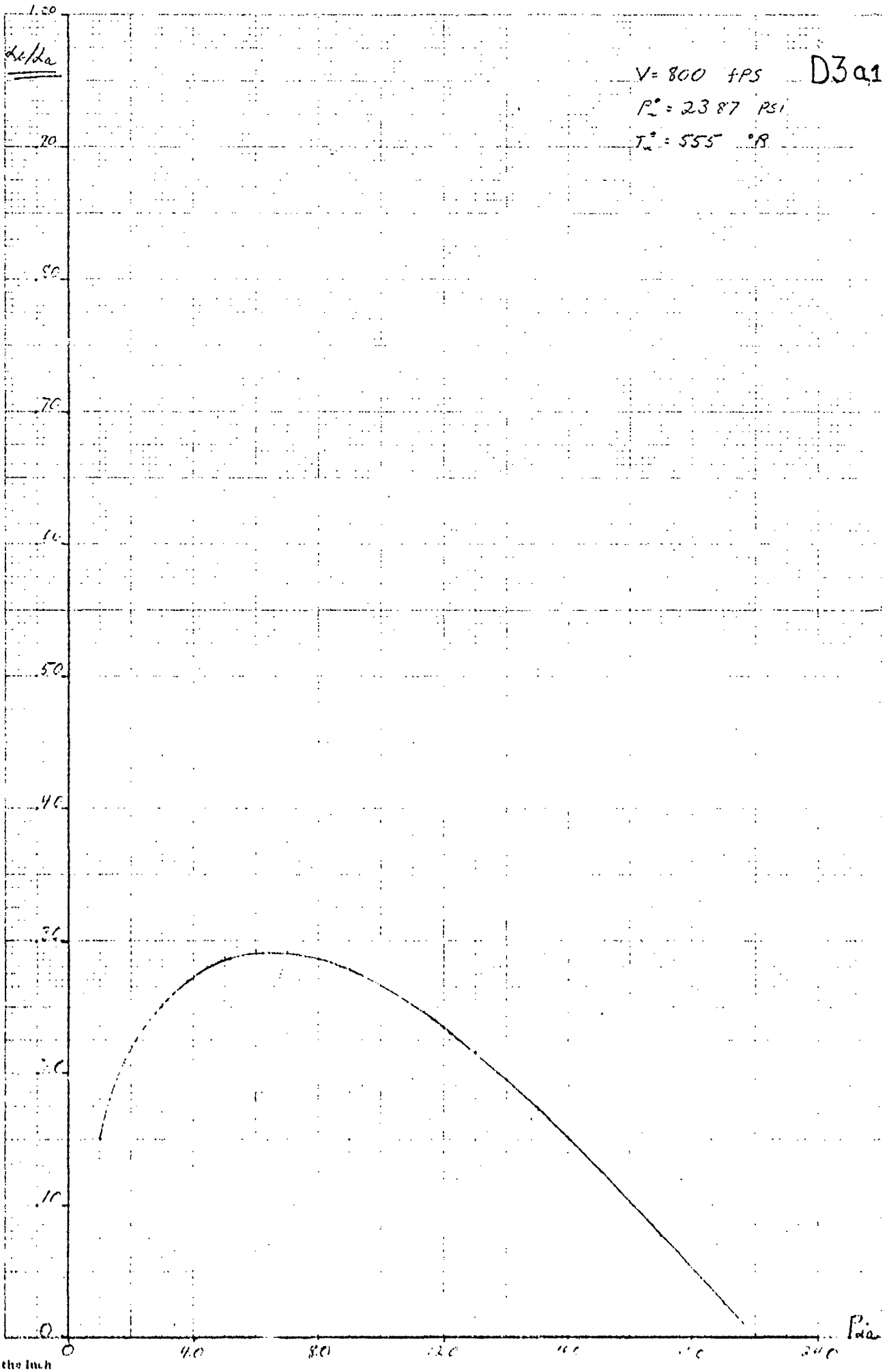

Squares to the Inch

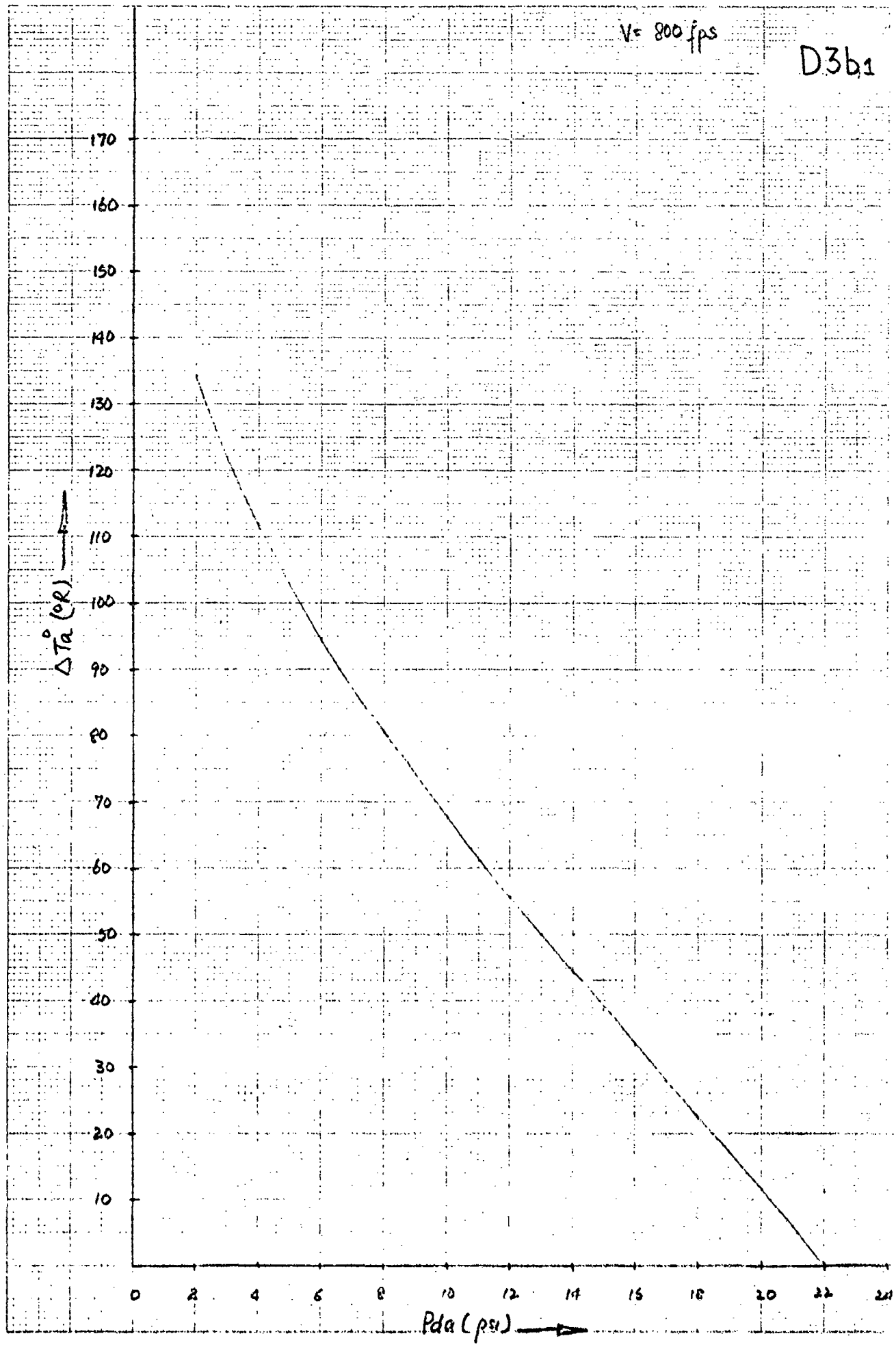
V= 800 fps
D3b1
170
160
150
140
130
120
110
100
90
80
70
60
50
40
30
20
10
ΔTa° (°R)
0
2
4
6
8
10
12
14
16
18
20
22
24
Pda (psi)

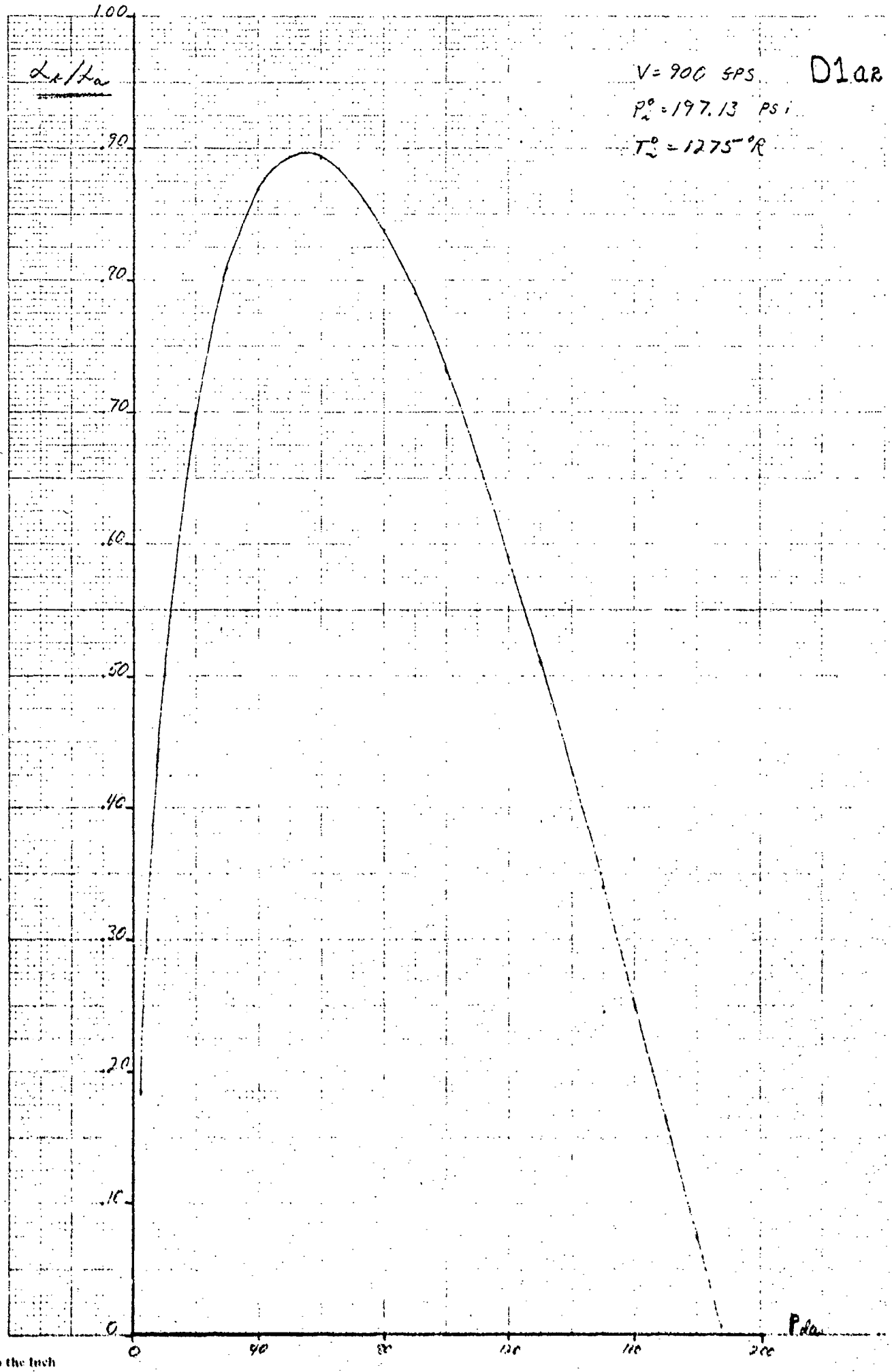

Squares to the Inch

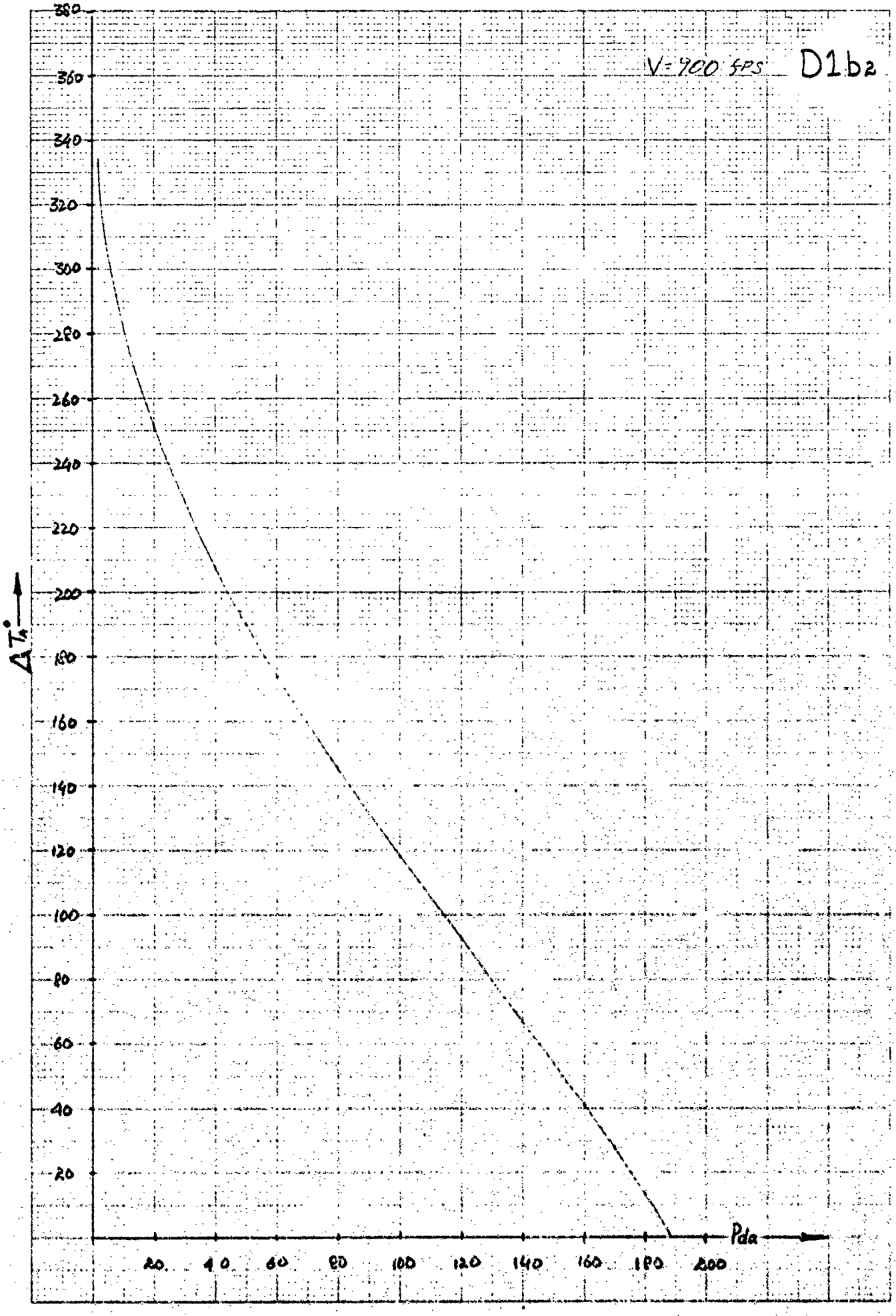

NATIONAL 12-282 Squares to the Inch

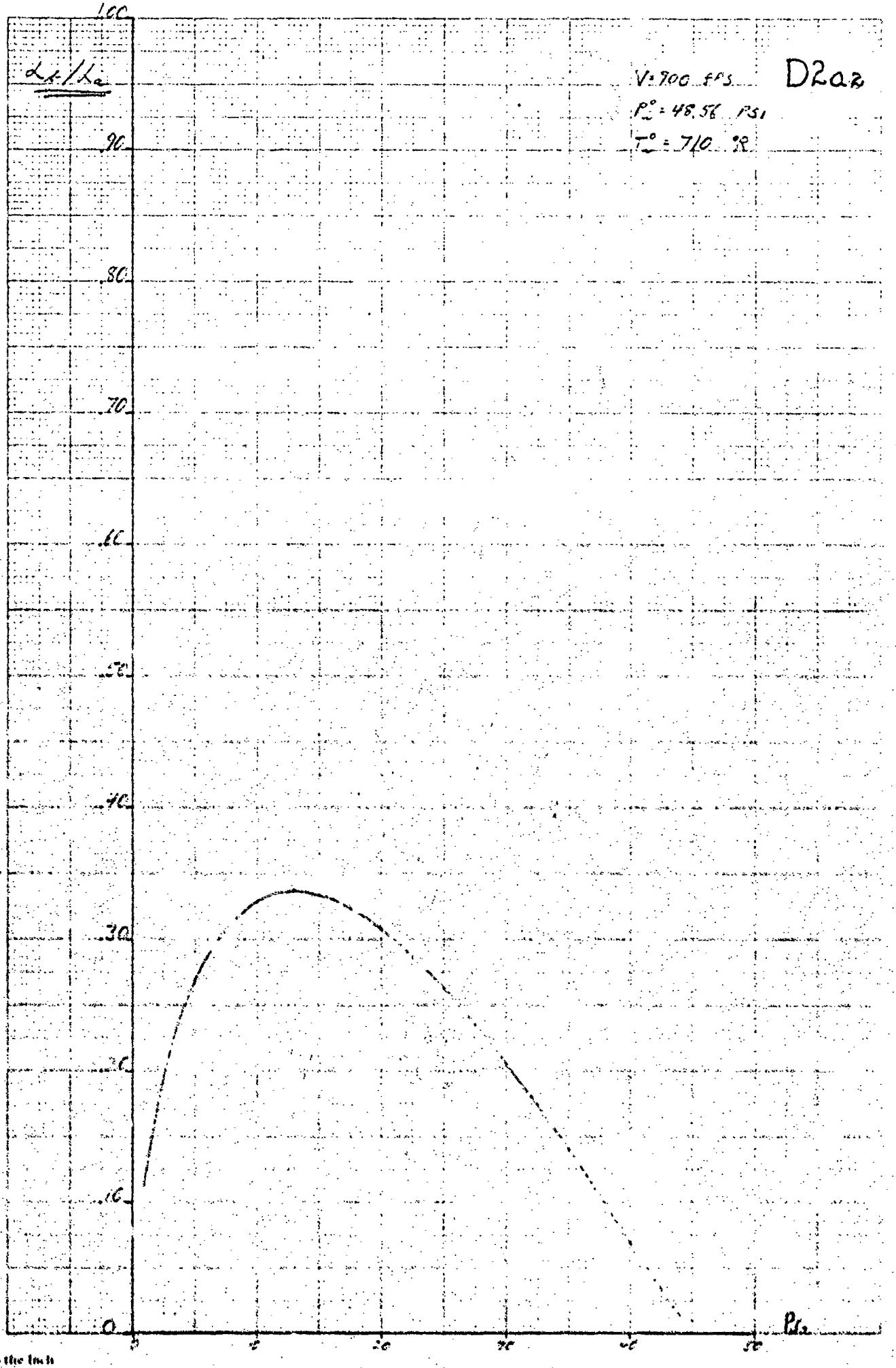

12-282
Squares to the Inch

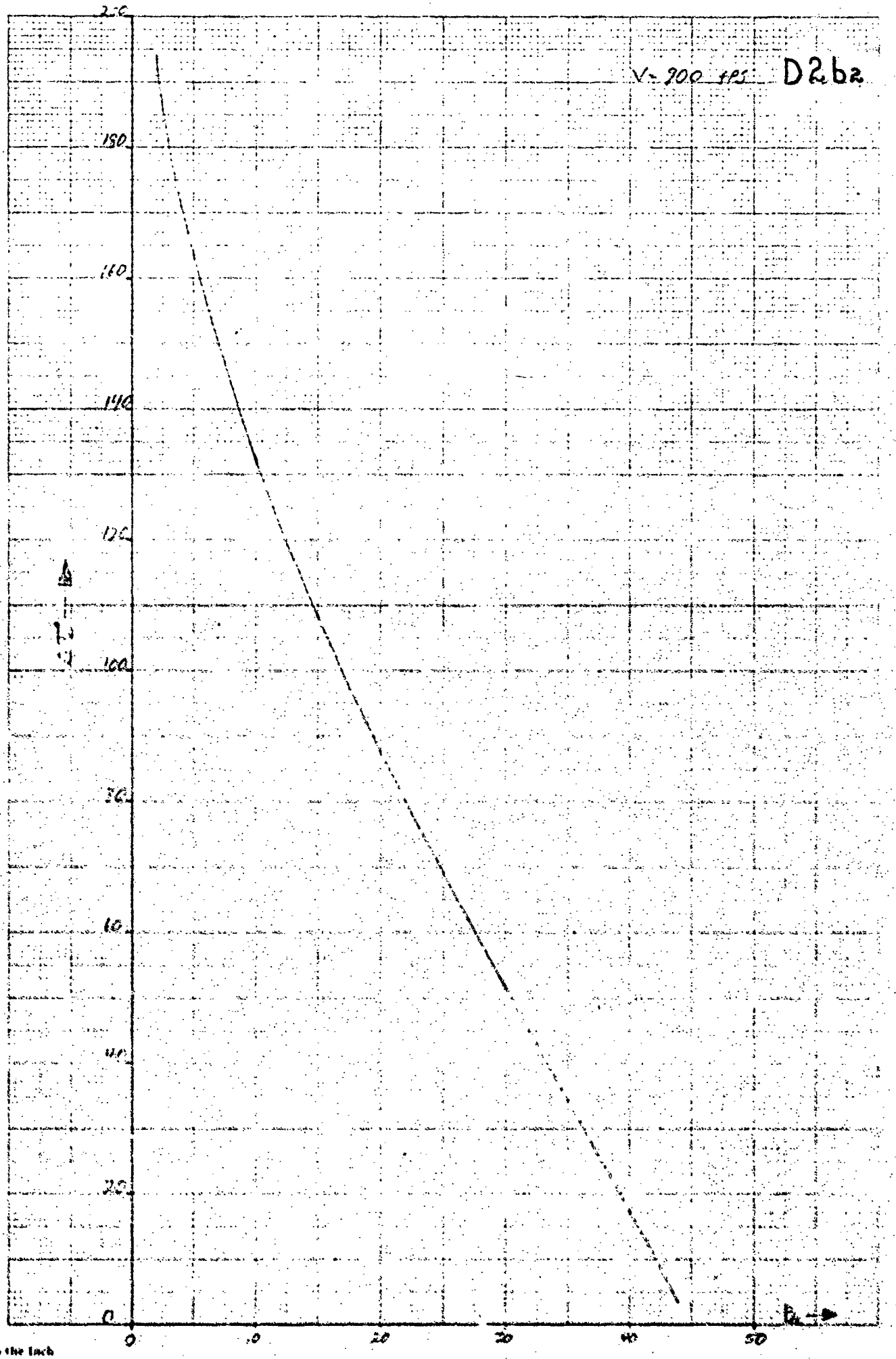

Squares to the Inch

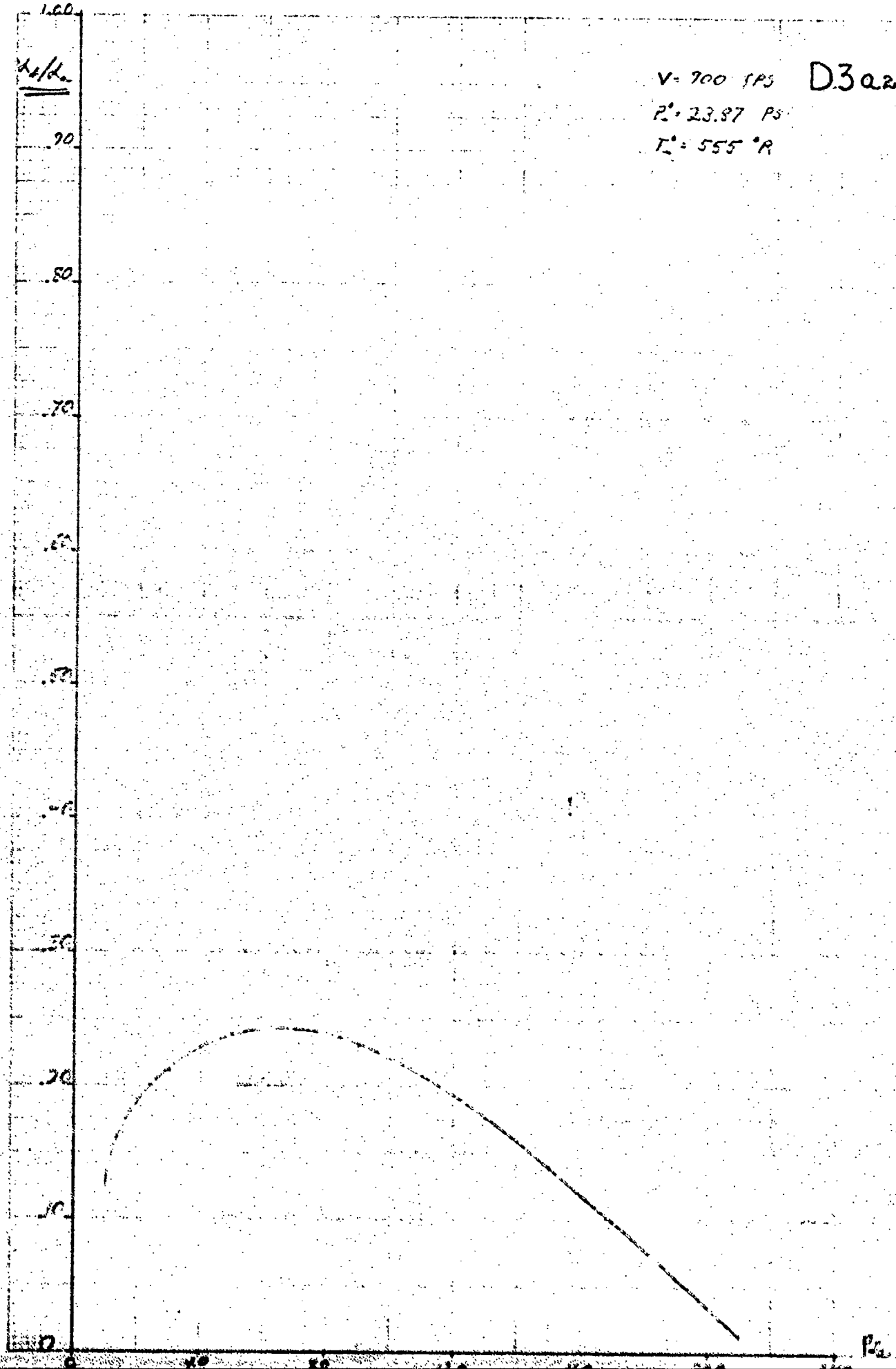

1.00
α_f/α_a
.90
.80
.70
.60
.50
.40
.30
.20
.10
0
V = 700 fps
D3a2
$P_a^* = 23.87$ psi
$T_a^* = 555$ °R
P_a

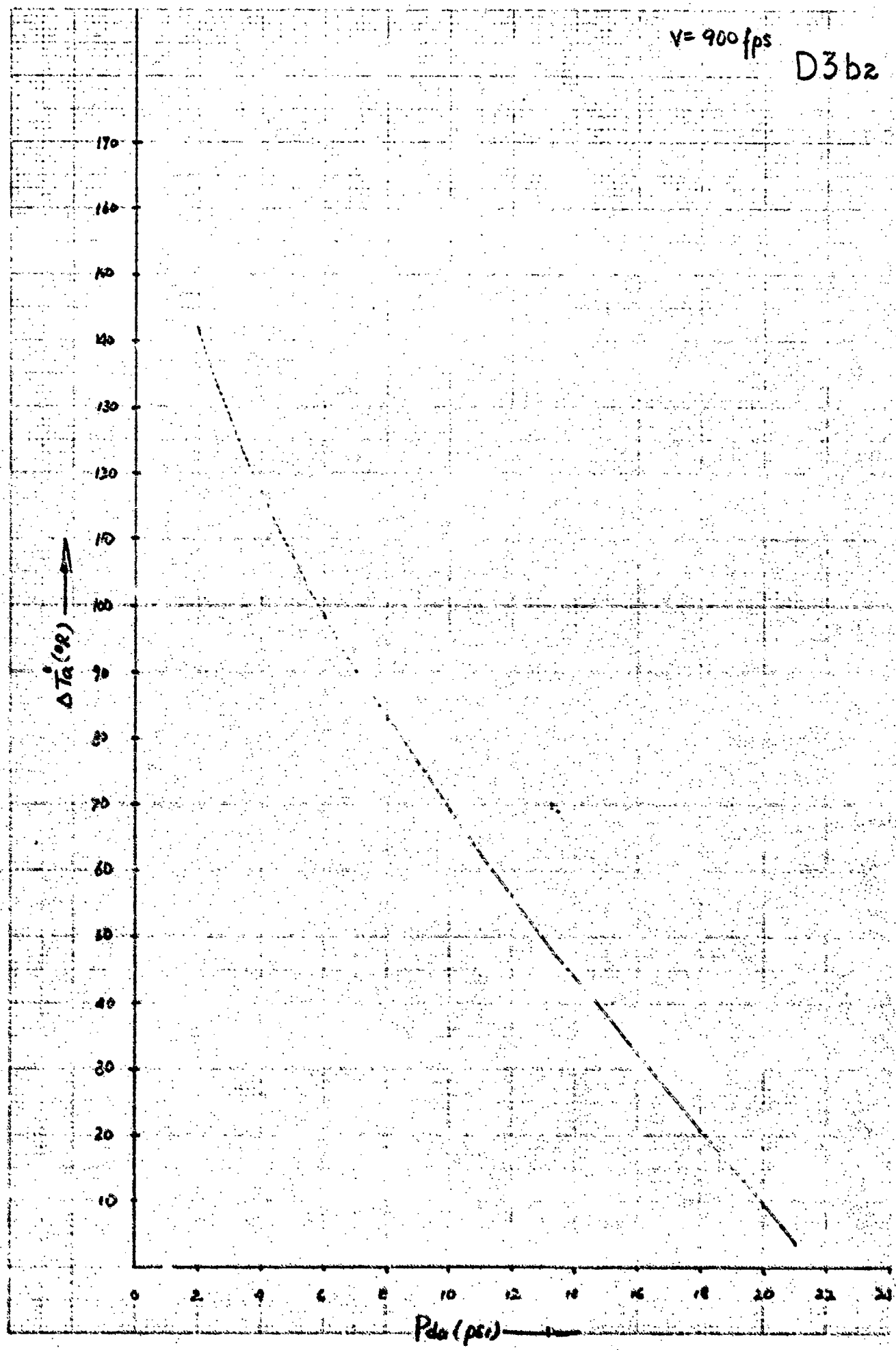
V= 900 fps
D3b2
170
160
150
140
130
120
110
100
90
80
70
60
50
40
30
20
10
ΔTa (°R)
0
2
4
6
8
10
12
14
16
18
20
22
24
Pda (psi)

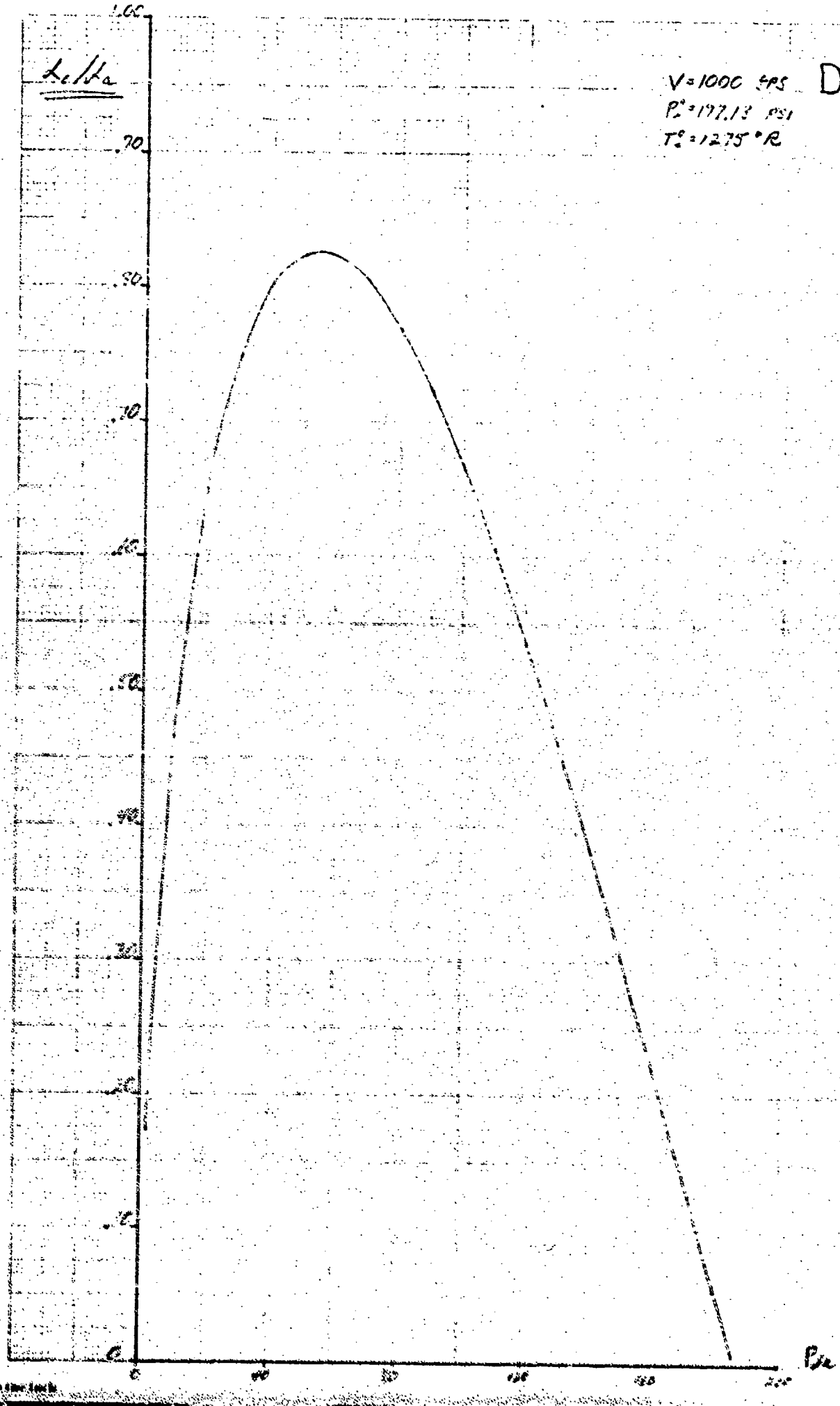

L_c/L_a
V=1000 fps
P_c^o=197.13 psi
T_c^o=1275 °R
D1a3
1.00
.90
.80
.70
.60
.50
.40
.30
.20
.10
0
0
40
80
120
160
200
P_{de}

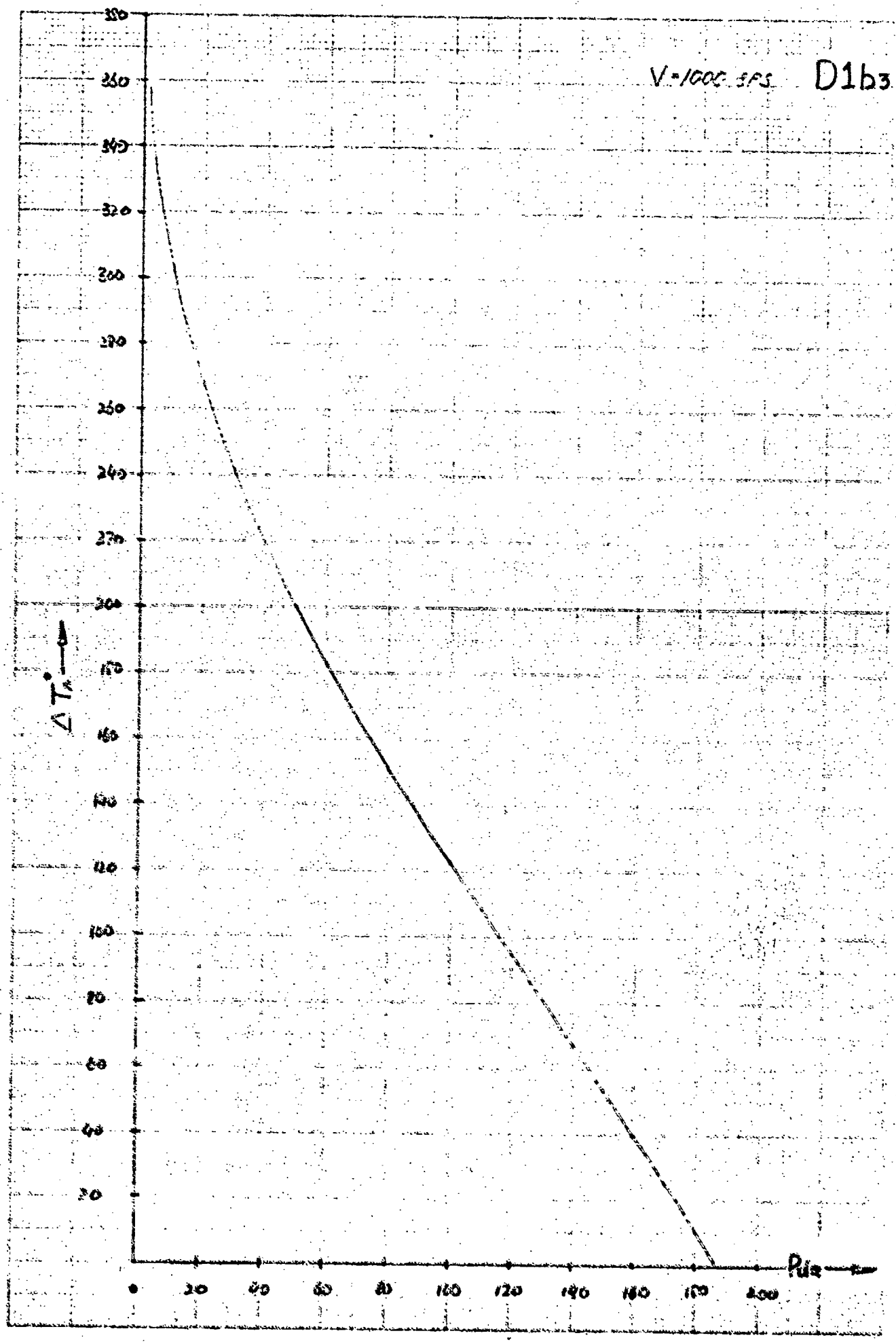

Squares to the Inch

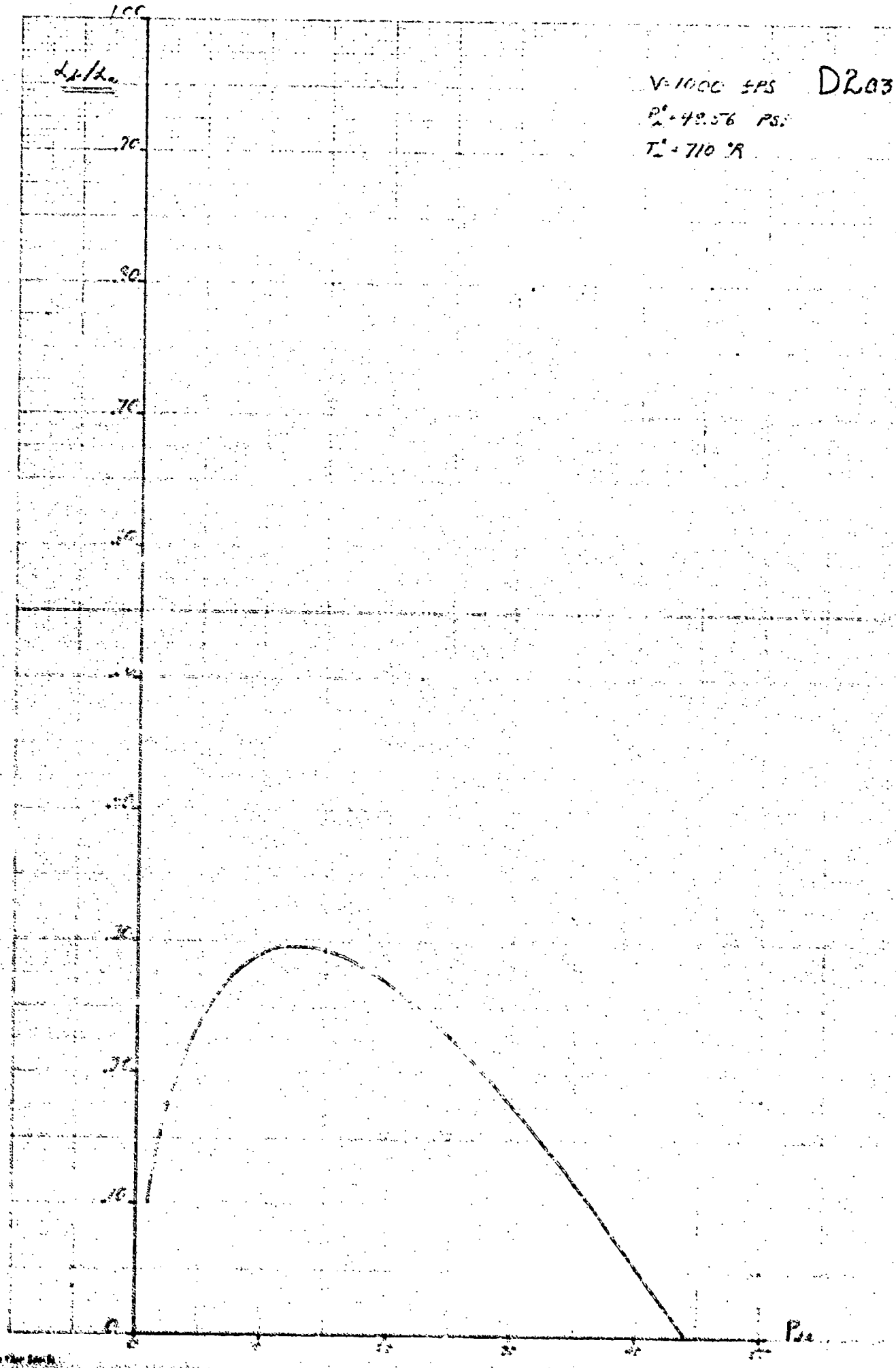

α_t/α_a
V=1000 fps
D203
P_a^0=49.56 PSI
T_a^0=710 °R
1.00
.90
.80
.70
.60
.50
.40
.30
.20
.10
0
P_{sa}

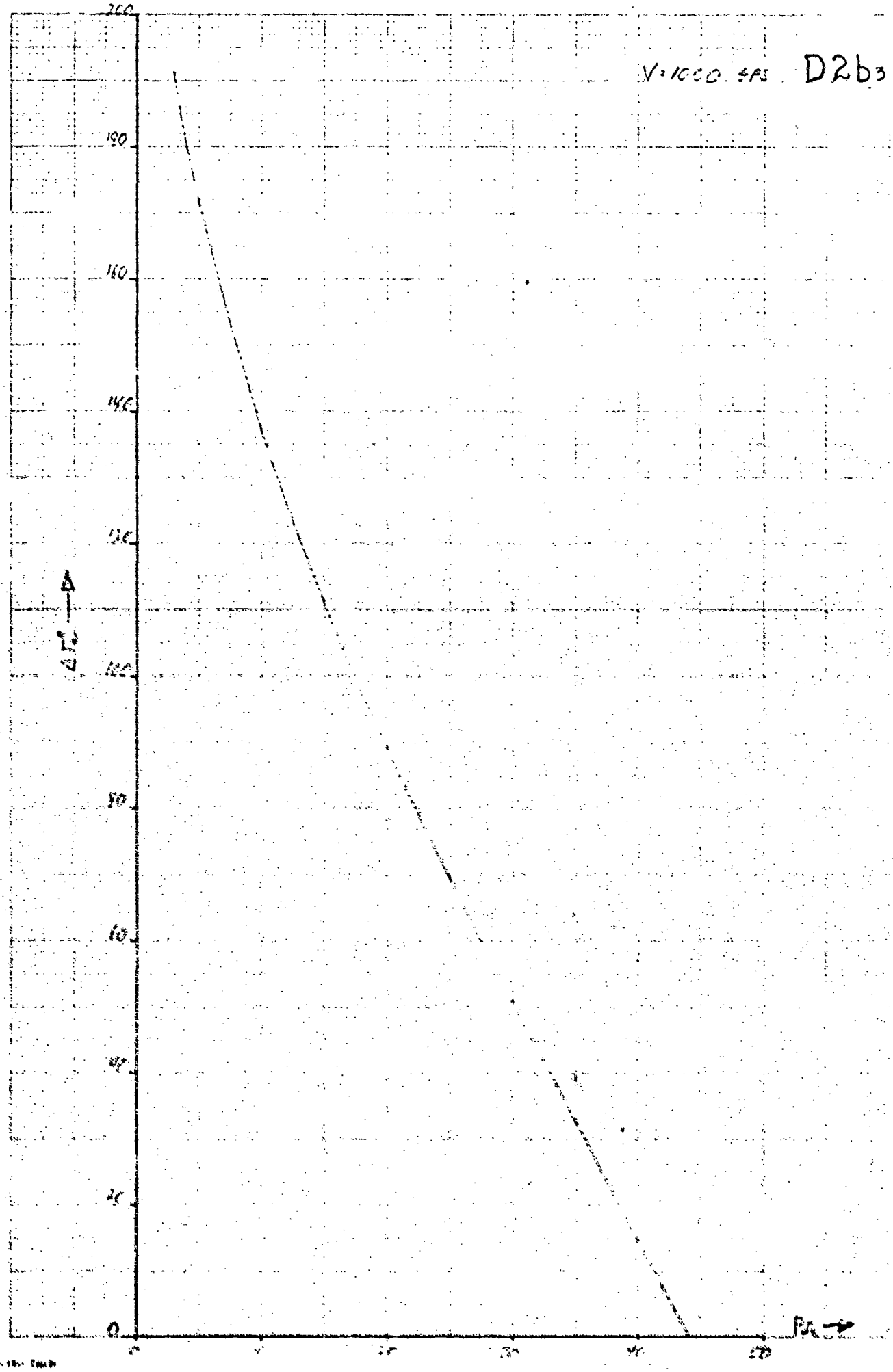
V=1000 FPS
D2b3
200
180
160
140
120
100
80
60
40
20
0
20
40
60
80
100

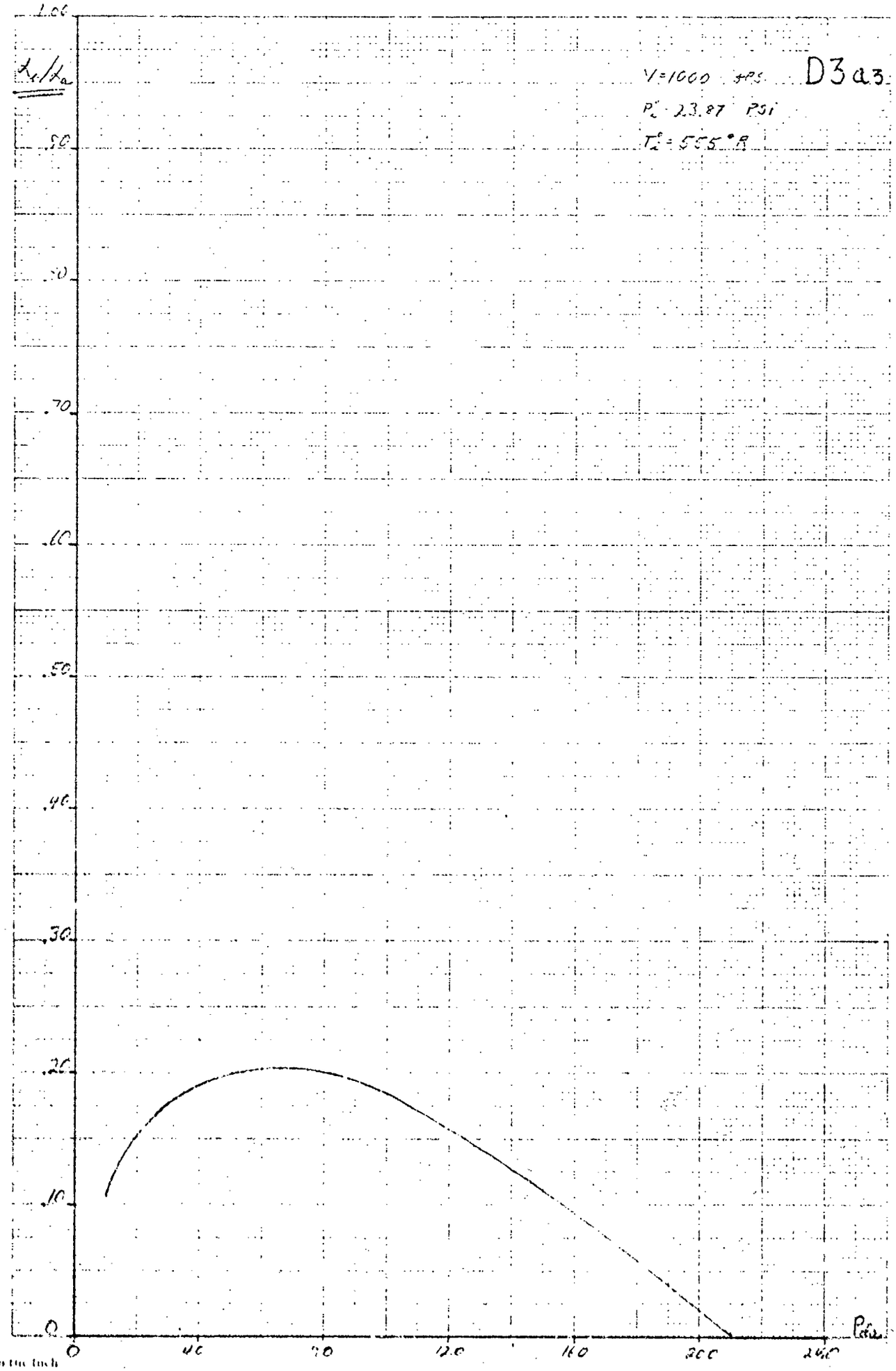

Squares to the inch

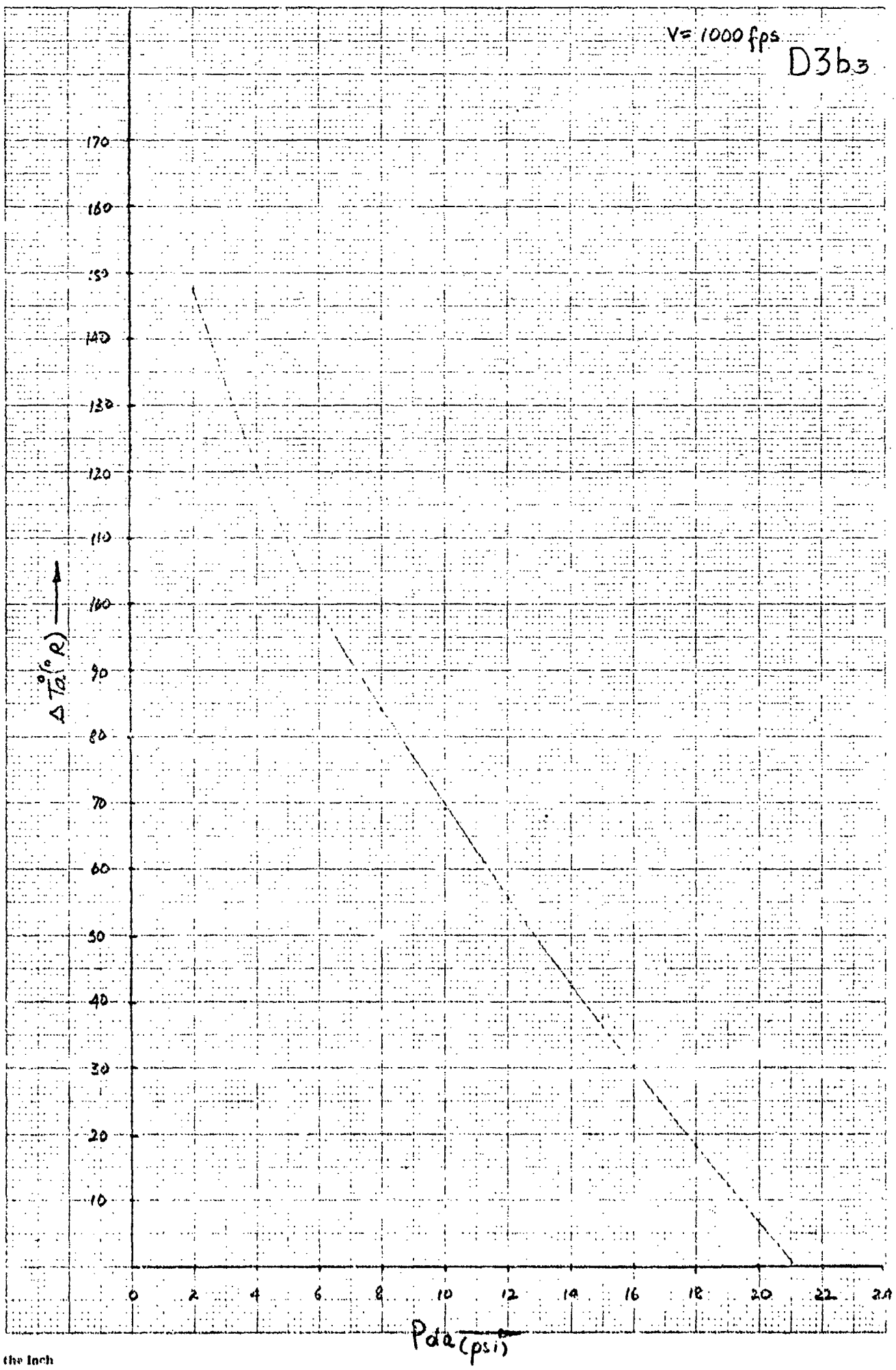

9 Squares to the Inch

APPENDIX SECTION E: EFFECT OF VARIATION OF p_{da} ON μ AND κ

Case 1 (V=800, 1000 fps)

Mass Flow Ratio vs. Cold Discharge Pressure

Cooling Capacity Coefficient vs. Cold Discharge Pressure

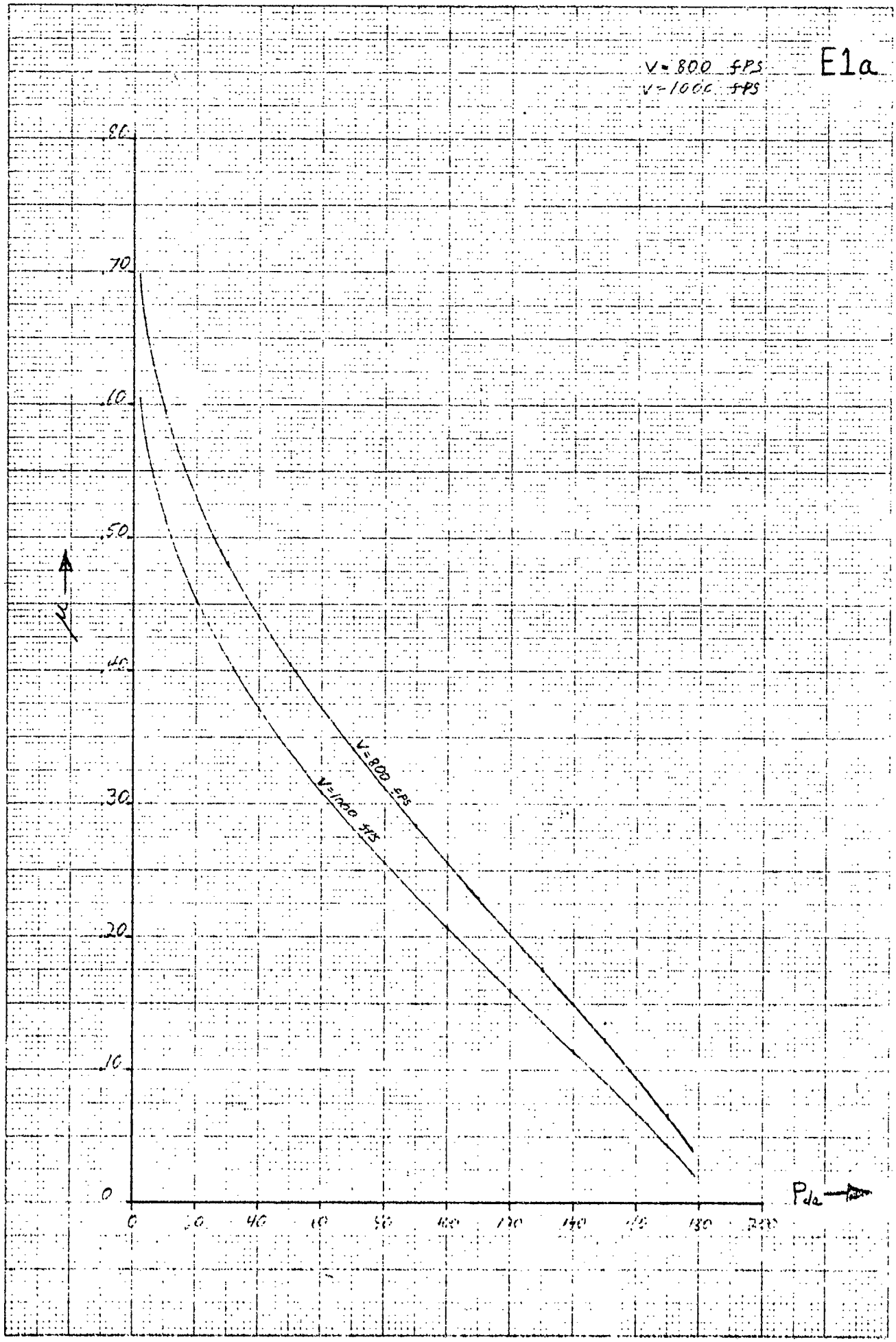

0 Squares to the Inch

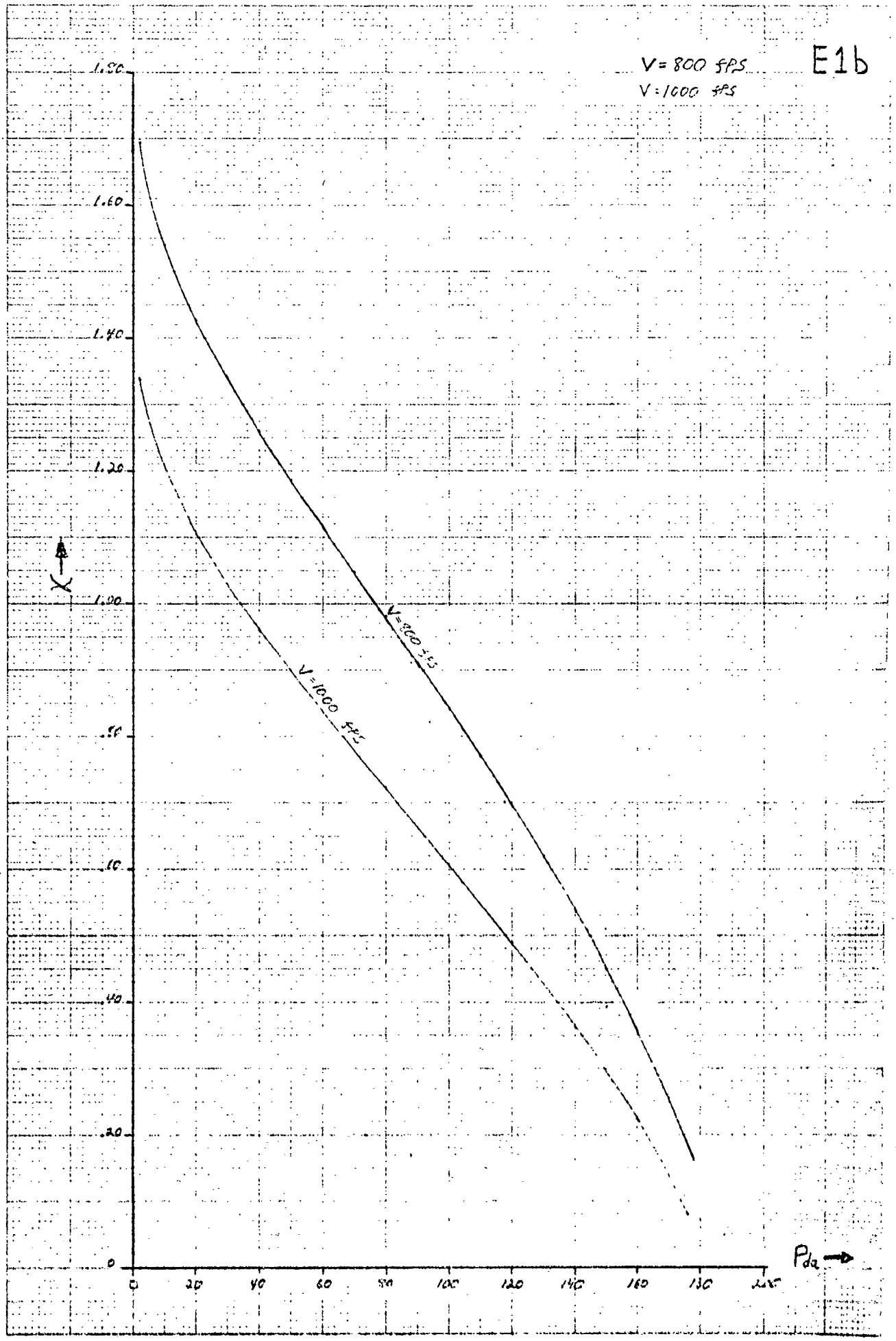
E1b
V = 800 FPS
V = 1000 FPS
1.80
1.60
1.40
1.20
1.00
.80
.60
.40
.20
0
X
V = 800 FPS
V = 1000 FPS
0
20
40
60
80
100
120
140
160
180
200
Pda